ELSEVIER

Catalysis Today 27 (1996) 497–532

CATALYSIS TODAY

# A case study: surface chemistry and surface structure of catalytic aluminas, as studied by vibrational spectroscopy of adsorbed species

Claudio Morterra *, Giuliana Magnacca

*Department of Inorganic, Physical and Materials Chemistry, University of Turin, via P. Giuria 7, I-10125 Turin, Italy*

**Abstract**

Transition phase aluminas have been used as catalysts, and their surface chemical properties have been studied for over 30 years. The various steps of the gradual comprehension of the surface structure and surface chemistry of aluminas are here summarized. Our main attention has been devoted to various aspects of the surface chemistry of aluminas, as revealed by the adsorption of selected probe molecules, rather than to a systematic description of the adsorption of the very many probe molecules used over the years. Among the various physico-chemical aspects of aluminas, some were thought to be of particular interest: solid (bulk) and surface vibrations, the surface hydrated layer, surface basicity and surface acidity. Whenever possible, a comparison between spectroscopic and quantitative data has been proposed.

*Keywords:* Infrared spectrometry; Aluminas; Surface chemistry and structure

## 1. Introduction

Should the term alumina be plainly used to designate 'the oxide of trivalent Al', in ordinary conditions it would be referred to the thermodynamically stable corundum phase, otherwise known as $\alpha$-$Al_2O_3$. The latter crystallizes in the hexagonal system [1] and is the ultimate product of the thermal treatment (at $T \geq 1400$ K) of all Al oxidic and/or Al hydrate systems [2].

In the practical use, the same term alumina is often employed to designate several quite different materials.

For instance, in the field of ceramic applications the term alumina is routinely employed both with reference to the various starting Al hydroxides, precursors of the actual $Al_2O_3$ ceramic and with reference to the ceramic corundum phase. All other intermediate oxides have virtually no interest for ceramists and are never referred to as aluminas nor are they reported in any detail in the diagrams, as they are metastable phases.

Unlike that in the field of catalytic applications the term alumina is also very common, but never referred to the precursors Al hydroxides nor to the hexagonal phase $\alpha$-$Al_2O_3$, catalytically inactive. In the practical language of catalysis and surface chemistry the term alumina is normally referred to the so-called transition aluminas. The latter are metastable phases of low crystallinity characterized by high surface area and open porosity; also for these reasons, though

* Corresponding author.


*SSDI* 0920-5861(95)00163-8

not only for these reasons, transition aluminas are the only Al oxides of practical interest for catalytic applications.

As this review is devoted to the surface and spectroscopic features of aluminas of major catalytic interest, we decided to concentrate our attention mainly on the most commonly used crystalline cubic transition phase $Al_2O_3$ systems and to neglect other less common systems like, for instance, amorphous aluminas and hexagonal-type aluminas ( $\chi$-$Al_2O_3$ and $\kappa$-$Al_2O_3$). Besides transition aluminas, also some of the features of Al hydrates and of the corundum phase will be necessarily mentioned every now and then. In fact, the structural and coordinative evolution of the Al oxide system from one extreme to the other will turn out to be quite important for the definition and comprehension of some of the surface properties of the transition phases. For these reasons, and to avoid confusion, for all the systems considered here we will use always either the complete phase designation (e.g., $\gamma$-AlOOH, $\theta$-$Al_2O_3$ and $\alpha$-$Al_2O_3$) or the current phase name (e.g., boehmite, transition aluminas and corundum).

The complex thermal evolution of the Al hydroxides ($Al(OH)_3$; gibbsite, bayerite and norstrandite) towards corundum, passing through the monohydrates (boehmite and pseudoboehmite) and the various transition alumina phases, has been thoroughly studied in the sixties by Lippens [2,3]. His detailed phase description is considered to be still valid and has been constantly referred to in all more recent studies carried out in the field (e.g., see [4–6]).

Scheme 1 presents synthetically the various pathways of the thermal evolution from Al hydroxides towards the corundum phase, as first proposed by Lippens and Steggerda [2].

As mentioned, catalytic aluminas belong to the group of transitional $Al_2O_3$ phases, (meta-) stable in the ca. 750–1370 K range. They are usually further divided in two families [7]: the so-called low-temperature transition phases ($\gamma$- and $\eta$-$Al_2O_3$) and the high-temperature transition phases ($\delta$- and $\theta$-A $l_2O_3$). On a crystallographic ground, the irreversible thermal transition from low- to high-temperature transition aluminas has been reported to be a continuous process [8], i.e., a mere transition of the order-disorder type [6,9,10]. In fact, the structural differences between the two families of aluminas are relatively small as all transition aluminas belong to the cubic system and have the

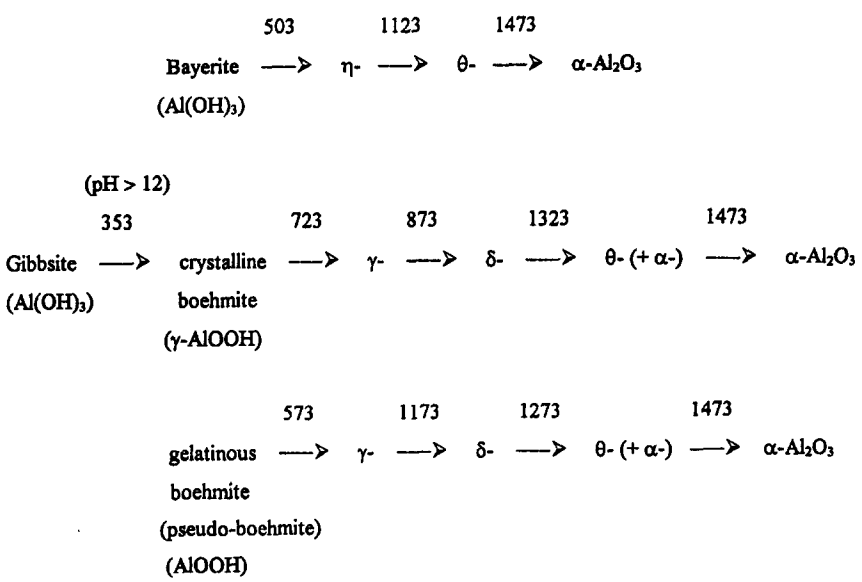


Scheme 1. Phase transitions from Al hydroxides to corundum (From Ref. [2]). The values above the arrows are temperatures (K).

nature of defective spinels. On a catalytic ground, the passage from low-temperature to high-temperature transition aluminas is more critical. In fact, the high-temperature transition phases are definitely less active than the low-temperature ones. This is not merely due to the lower surface area of the former ones (brought about by the higher order and larger particle size), but must reflect a different population of surface active sites. IR data to be reported and discussed below will justify, at least in part, this expectation.

Spinels are the mixed oxides of $Al^{3+}$ (and, possibly, of other trivalent cations) with divalent cations and have the general formula $MAl_2O_4$: their name derives from the natural spinel mineral $MgAl_2O_4$. In normal spinels, i.e., systems in which no inversion phenomena occur (inversion as observed, for instance, in $NiAl_2O_4$), the $M^{2+}$ cations occupy only one-eighth of the tetrahedral sites in the cubic close packed array of oxide ions, whereas $Al^{3+}$ (or other possible trivalent cations) occupy half of the octahedral sites, so that the general formula is often written as $M^{IV}[Al_2^{VI}O_4]$ or, with reference to the unit cell, $M_8^{IV}[Al_{16}^{VI}O_{32}]$.

The defective nature of the transition alumina spinels derives from the presence in aluminas of only trivalent cations, so that some of the lattice positions occupied by cations in mixed-oxide spinels must remain empty to guarantee electrical neutrality. The overall formula referred to the unit cell is then $Al_8^{IV}[Al_{13\ 1/3}^{VI}\square_{2\ 2/3}O_{32}]$. The square symbol denotes the presence of cationic vacancies with respect to the ideal spinel structure: this notation implies, as suggested by Wilson and McConnell for $\delta$-$Al_2O_3$, that cation vacancies are essentially located in octahedral sites, but vacancies should be more realistically imagined as distributed randomly between tetrahedral and octahedral cavities [8].

It is also logical to expect some of the vacant cationic positions, imposed by the $Al_2O_3$ stoichiometry, to be present also in the surface layer of transition aluminas. This is certainly one more factor, besides the double coordination presented by Al ions, that is bound to be somehow responsible for the complex and variable surface situation typical of the transition alumina systems.

To conclude this introduction section, it is important to remark that not only (intrinsic) structural and coordinative factors contribute to the complex and variable spectral features of transition aluminas, but also (incidental) chemical factors do. In fact, it is known that little amounts of some contaminants (e.g., alkali metal ions) may modify to a large extent the surface layer of aluminas and consequently the spectral behavior of the systems. For this reason, in this review we will try to do our best to report mainly data relative to either high purity alumina preparations obtained on a laboratory scale or to commercial aluminas, whose purity is known and/or reported by the authors.

## 2. Vibrational modes of the solid and surface vibrations

The fundamental vibrations of solids are localized in the low frequency region of the IR spectrum ($\tilde{\nu} < 1200\ cm^{-1}$). n the usual surface chemistry work, normally based on the in situ use of self-supporting pellet samples, these modes remain totally non accessible. In fact, the intensity of these vibrational modes is so high that they represent a virtually complete spectral cut-off for the solid, even when very thin pellets or thin-layer deposition samples are used.

If, on the other hand, optically thin KBr or CsI pellet samples are used (this is a common practice in analytical vibrational spectroscopy), the low $\tilde{\nu}$ region of the spectrum does indeed become optically accessible, but in these conditions no reliable adsorption–desorption surface chemistry experiments can be carried out. As a consequence, in most cases the surface component(s) of the vibrational modes of a solid cannot be singled out and their modifications during adsorption–desorption processes cannot be observed. In this respect, as we shall see below,

aluminas represent to some extent a fortunate exception.

### 2.1. Vibrations of the solid

Fig. 1 reports the IR spectra of the fundamental modes of several Al oxidic systems; Fig. 1A is taken from a recent work by Busca et al. [11] and concerns KBr-pellets of the phases $\gamma$-$Al_2O_3$ (a), $\theta$-$Al_2O_3$ (b) and $\alpha$-$Al_2O_3$ (c), whereas Fig. 1B shows, for comparison, original KBr-pellet spectra of $\delta$-$Al_2O_3$ (d), $\eta$-$Al_2O_3$ (e) and $\gamma$-AlOOH (f).

The spectra of Fig. 1 confirm that: (i) whenever the sole octahedral coordination of Al ions is present, like in corundum and boehmite (c, f), the spectrum is dominated by the strong stretching mode of 'condensed' $AlO_6$ octahedra [12], centered in the region 750–600 $cm^{-1}$. The absorption may be split into more components (two in the case of $\alpha$-$Al_2O_3$ [12] and three in the case of $\gamma$-AlOOH [13]), due to lowering of the local symmetry and resolution of degenerate modes, but no strong absorptions are ever observed at $\tilde{\nu} > 800$ $cm^{-1}$; (ii) whenever also the tetrahedral coordination of Al ions is present, like in the transition alumina phases (a, b, d and e), there is also a strong and broad absorption in the region 900–750 $cm^{-1}$, due to stretching vibrations of a lattice of interlinked ('condensed') tetrahedra [12]. In particular, in the case of the high-temperature spinel transition phases the band of the $AlO_4$ tetrahedra becomes broader, stronger and partly resolved into several sharp components, due to the higher crystalline order achieved [10]. This can be observed with the $\delta$-$Al_2O_3$ preparation (see spectrum d of Fig. 1) and, even more, with the $\theta$-$Al_2O_3$ phase (see spectrum b of Fig. 1 and the spectrum of a fairly pure $\theta$-$Al_2O_3$ preparation reported by Tarte in Ref. [12]).

### 2.2. Surface vibrations

The strong lattice modes of Al oxides shown in Fig. 1 certainly contain also contributes de-

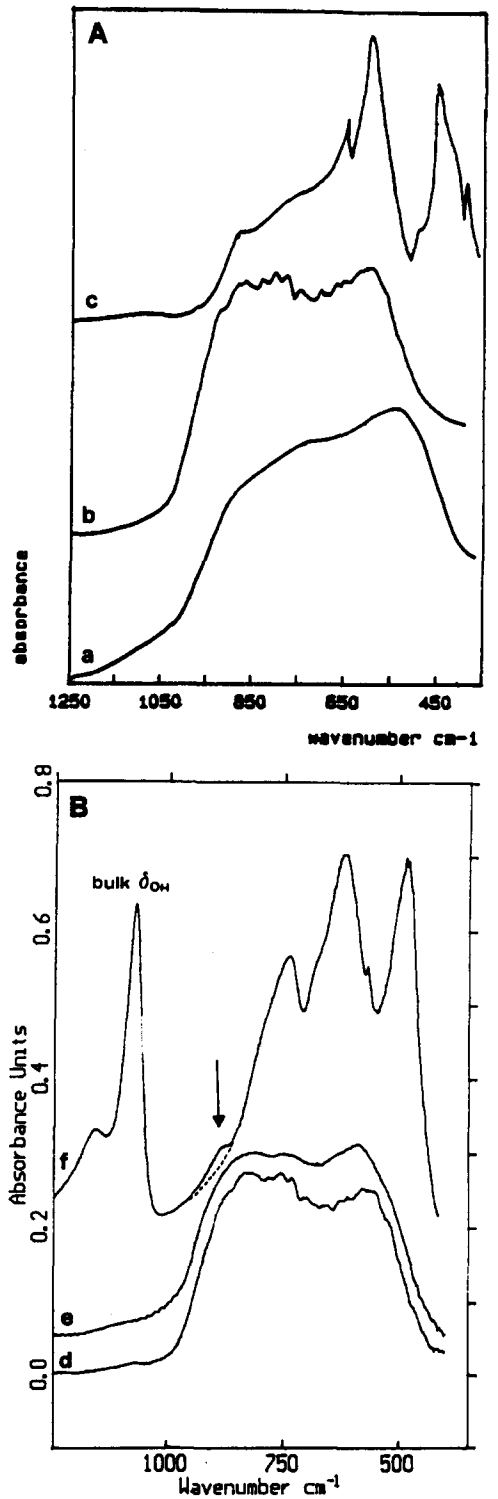


Fig. 1. IR spectra in the skeletal region of some Al oxide preparations. Section A: $\gamma$-$Al_2O_3$ (a), $\theta$-$Al_2O_3$ (b), $\alpha$-$Al_2O_3$ (c) (from Ref. [11]). Section B: $\delta$-$Al_2O_3$ (d), $\eta$-$Al_2O_3$ (e), $\gamma$-AlOOH (f).

riving from the part of the relevant vibrations that concern Al and O atoms in the surface layer. Especially in the case of high surface area materials, the fraction of the fundamental modes that mainly involves the surface layer is expected to be quite large, but the spectral location of these surface vibrational components is hard to predict, as nothing is known a priori on the change (if any) of the lattice force constants in the surface layer.

In the case of the crystalline γ-AlOOH system, spectrum f of Fig. 1B presents a weak band at ca. 900 $cm^{-1}$, marked with an arrow in the figure. In a recent paper devoted to the surface characterization of boehmite and pseudo-boehmite [14], it has been shown that the band at ca. 900 $cm^{-1}$ is due to vibrational modes localized in the surface layer and most likely involving the deformation of surface OH groups. In fact, from in situ spectra of non-supported boehmite the band at ca. 900 $cm^{-1}$ turns out to be perturbed by adsorption phenomena, to shift to lower frequency upon dehydration (as expected of a $\delta_{OH}$ mode that becomes free from H-bonding), and to shift downwards outside of the observable spectral range upon surface exchange with $D_2O$. The observation of this surface-localized vibration has been possible, in the case of the AlOOH system, as a consequence of the large displacement of the vibrational frequency with respect to the corresponding bulk mode(s); in fact, surface OH groups are expected to be chemically very different from bulk OH groups, and the relevant vibrational force constants are thus expected to be very different.

It is quite interesting that the observation of surface-localized vibrational modes, different from OH modes, has been possible also in the case of high-area transition alumina phases. In fact:

(i) In 1976, Morterra [15] first reported that the adsorption on highly dehydrated transition aluminas of a strong base like pyridine brings about an appreciable increase of IR transparency on the high frequency side of the alumina cut-off. This effect was interpreted as due to the relaxation of some Al-O vibrations localized in the surface layer and absorbing in the spectral region around 1000 $cm^{-1}$ [15,16].

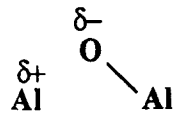


Scheme 2. Surface defective structure in highly dehydrated aluminas, responsible for a surface-localized vibrational state (from Ref. [17]).

(ii) In 1984, Lavalley and Benaissa [17], using accurate in situ experiments and differential absorbance spectra, could show that dehydration of aluminas at increasingly higher temperatures does actually create a discrete band, weak and broad, centered at ca. 1050 $cm^{-1}$, as predicted by previous works [15]. The band was ascribed to an Al–O vibrational mode localized in strained groups of the type described in Scheme 2.

The surface defect would be created during high temperature surface dehydroxylation. The defect was also supposed to be readily destroyed upon rehydration of the alumina, as demonstrated by a simultaneous disappearance of the weak band at ca. 1050 $cm^{-1}$ upon water adsorption [17].

(iii) More recently, Marchese et al. [18] and Morterra et al. [19] confirmed the identification of a surface-localized Al–O vibrational mode on both low- and high-temperature transition aluminas. It was also shown that no severe surface chemical changes (like, for instance, the rupture of a strained Al–O bond) are actually needed to have the $\nu_{Al-O}$ vibration shifted downwards. The differential absorbance spectra reported in Fig. 2 show that, upon the reversible adsorption of a soft base like CO, a complex band localized in the 1100–1000 $cm^{-1}$ range is gradually and reversibly eliminated.

It is known that, on highly dehydrated aluminas, the adsorption of CO does not cause the rupture of bonds, but just a polarization or weak σ-coordination onto unsaturated surface cations,

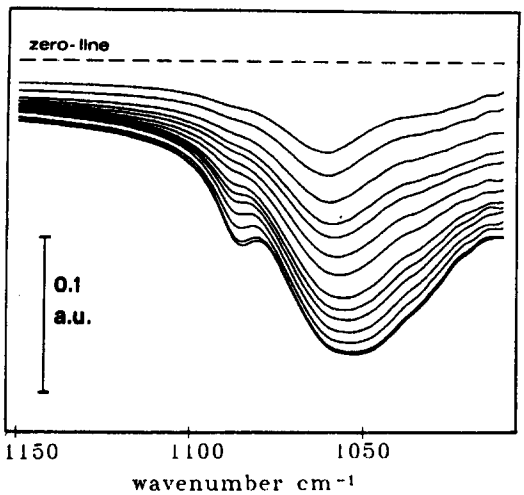


Fig. 2. Differential absorbance spectra showing the elimination of surface-localized vibrational states upon adsorption of CO at 77 K onto $\gamma$-$Al_2O_3$ activated at 1023 K (from Ref. [19]).

as will be described in more detail in a following section.

The complex band at ca. 1050–1100 $cm^{-1}$ has been interpreted as due to some spinel $Al^{IV}$–O stretching modes localized at the surface; they would be shifted upwards with respect to the regular bulk $Al^{IV}$–O stretching mode(s), that absorb at ca. 850 $cm^{-1}$ as shown in Fig. 1, and the shift would be caused by the surface increase of covalency and decrease of the Madelung energy, brought about by crystal truncation and surface dehydration [19]. Upon gas/solid adsorption, ligands are added to the coordination sphere of surface cations, the overall coordination of surface ions increases, and the covalency of the surface decreases. As a consequence, the surface-localized $Al^{IV}$–O vibrational states shift downward toward the regular spectral position of bulk $Al^{IV}$–O vibrations and outside of the spectral range observable in the in situ transmission mode.

If a weak adsorbate like CO causes the downward shift of surface-localized vibrational states, all adsorption processes are expected to do the same, including the strong adsorption of pyridine (as first observed by Morterra [15]), and the dissociative uptake of water that rebuilds the surface hydrated layer and, doing so, destroys surface defects (as reported by Lavalley and Benaissa [17]).

## 3. Surface hydroxyls

The surface of a solid, either massive or microcrystalline, can be regarded as an extended defect. In fact, a 'neutral' truncation of the crystals that leaves on either side an even number of electrical charges and originates the surface termination of the solid, leaves in the uppermost layer(s) anions and cations that are coordinatively unsaturated (cus). For this reason, when exposed to the atmosphere, all solids become covered of various types of adsorbed species whose role is to compensate, at least in part, the surface unsaturation brought about by the crystals truncation.

In the case of metal oxides, the outer layer is usually made up of different adsorbed species, whose nature is at least in part related to the preparative history of the material (carbonates, nitrates, hydrocarbonaceous residues are most common). But by far the most abundant component of the surface layer of non-basic oxides is made up of water. Besides physisorbed water, adsorbed water can be present at the surface in the form of undissociated coordinated $H_2O$ species (in the case of some oxides like, for instance, titania this component can represent as much as ca. 50% of the surface layer), and in the dissociated form of surface hydroxyls.

The O–H stretching fundamental vibrations ($\nu_{OH}$) of OH groups located at the surface of oxides are readily observed in the high frequency region of the IR spectrum ($\tilde{\nu} \geq 2500$ $cm^{-1}$) [20]. When deriving from isolated groups (i.e., groups free from interactions of the H-bonding type), the bands due to O–H vibrations are sharper, relatively weak and located in the highest wavenumbers section of the high wavenumbers region (usually, $\tilde{\nu} \geq 3600$ $cm^{-1}$). For this reason, the spectral patterns of free surface hydroxyls are a spectral fingerprint of

the parent oxide, and very often yield a valuable criterium for the structural understanding of the surface layer of the solid [21].

The vibrational spectrum of surface hydroxyls of catalytic aluminas is complex and quite typical; it has been considered as unique since the earliest days of the IR technique applied to surface species. In fact, none of the known metal oxides presents, in the $\nu_{OH}$ spectral region, (i) the multiplicity of spectral components and (ii) the virtually constant spectral shape exhibited by transition aluminas dehydrated at medium-high temperatures ($T = 700–1000$ K).

An example of this complex and virtually 'constant' spectral shape is reported in Fig. 3, where curves b–d are relative to transition aluminas: in the range 3850–3550 $cm^{-1}$ there is a complex of 4–7 closely overlapped bands, that have been variously attributed to free or quasi-free surface OH groups.

It is quite evident that the OH spectrum of transition aluminas (curves b–d) is very different from that of the Al hydrate phase (curve a) and of the corundum phase (curve e), whereas a more complex and virtually constant spectrum is obtained from different transition aluminas isolated in similar conditions; minor, though not negligible, intensity differences are noted between low-temperature aluminas (curves b–c) and high-temperature aluminas (curve d).

The average position of the OH bands, as observed on various transition aluminas and in various thermal activation conditions, is reported in the first two columns of Table 1.

The assignment of the OH spectrum of transition aluminas has been for long time a hard and controversial task: it covered a period of over 30 years and in some respects it is not completely concluded yet. The multiplicity of bands made the job difficult: in the years, there have been several efforts while several physical

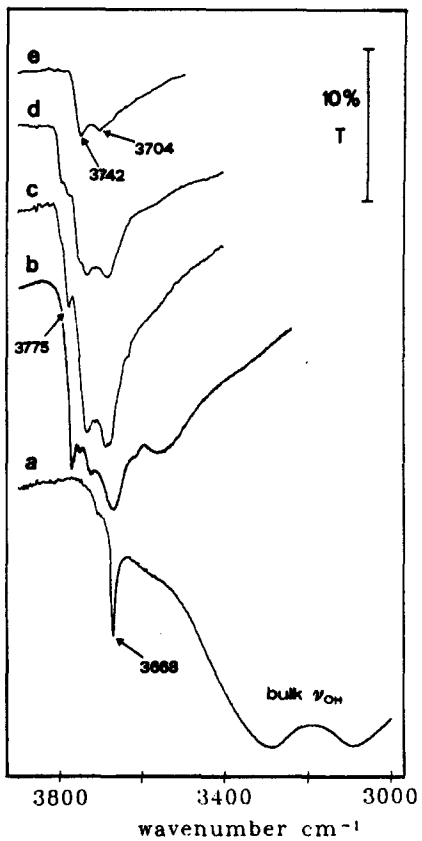


Fig. 3. The high wavenumbers region of the OH spectrum of some Al oxides. (a): γ-AlOOH activated at 300 K. (b–e): η-$Al_2O_3$, γ-$Al_2O_3$, θ-$Al_2O_3$ and α-$Al_2O_3$ activated at 773 K.

Table 1
Spectral position and assignments proposed for surface hydroxyl species on transitions aluminas

| OH band | Average frequency | Peri's assignment [22] | Tsyganenko's assignment [21] | Knözinger's assignment [35] | Busca's assignment [23] |
|---|---|---|---|---|---|
| 1 | 3800 | A | I | Ib | $Al^{IV}$ |
| 2 | 3775 | D | I | Ia | □-O-$Al^{IV}$ |
| 3 | 3745 | B | II | IIb | $Al^{VI}$ |
| 4 | 3730 | E | II | IIa | □-O-$Al^{VI}$ |
| 5 | 3710 | C | III | III | bridged |
| 6 | 3690 | C | III | III | bridged |
| 7 | 3590 | H-bonded | | H-bonded | tribridged |

and/or chemical parameters have been considered in various instances as responsible for the multiplicity of OH lines observed.

### 3.1. The role of nearest oxide neighbors. Peri's model

The first attempt to explain the complex OH spectrum of catalytic aluminas is due to the pioneering work of Peri [22].

He considered that: (i) the favored termination of the alumina crystallites is along the (100) plane, i.e., the face yielding the highest density of anions; (ii) up to ca. 770 K, the thermal dehydration of a fully hydroxylated surface occurs statistically by the condensation of adjoining OH pairs, avoiding the formation of multiple cus anion and/or cation sites. This process corresponds to the ordered elimination of ca. 2/3 of the surface layer and still leaves at the surface abundant adjacent hydroxyls that remain involved in H-bonding interactions; (iii) the elimination of all OH pairs is achieved by degassing at up to ca. 950 K (ca. 90% dehydroxylation) and creates 'defective' sites, i.e., sites made up of clusters of cus cations and/or anions; (iv) also isolated OH groups remain at the surface, corresponding to the residual ca. 10% of the surface hydrated layer: the $\nu_{OH}$ frequency of these isolated OH groups, that remain at the surface after the high temperature treatment, is determined by the number of nearest oxide neighbors, in that, the higher the number of nearby anions the higher is the $\nu_{OH}$ frequency.

Peri concluded that there are five possible free OH configurations. These are depicted in Fig. 4 and their symbol and frequency are reported also in the third column of Table 1.

If one considers that until very recent years nobody considered the 7th OH band (centered at ca. 3590 $cm^{-1}$) a free OH species [23], Peri's model could indeed explain virtually all of the spectral features of the OH pattern of transition aluminas. In fact, there was a nice correspondence between the number of OH configurations expected and the number of OH bands observed. This model was accepted as valid for many years.

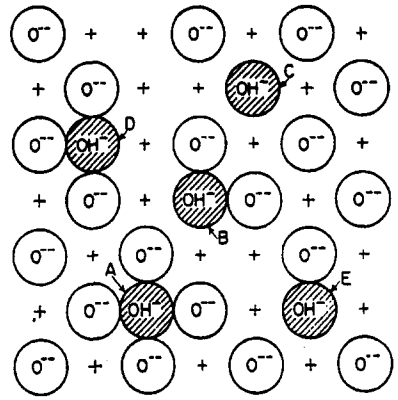


Fig. 4. Five types of isolated hydroxyl ions on partly dehydroxylated alumina. + denotes $Al^{3+}$ ions in lower layer (from Ref. [22]).

The major limit of Peri's model consists in the assumption of the (100) crystal face as the only possible termination for aluminas crystallites. This assumption yields an oversimplified picture of the spinel structure, in that only $Al^{VI}$ ions would result present in the uppermost layer and all OH groups in the fully hydrated surface (located on top of equivalent cations) would result to be equivalent. In these conditions, the adoption of a random elimination of water from adjoining OH groups is correct and no acidity–basicity concepts associated with different surface OH species needs to be involved. The model is thus valid, in principle, but gives only a partial description of the structurally complex situation of transition aluminas.

Another minor limit of Peri's model is that the defective spinel nature of aluminas was not taken into account: even if the sole (100) crystal face is considered and thus only $Al^{VI}$ cations result exposed, the one-to-one ratio between anions and cations does not correspond to the $Al_2O_3$ stoichiometry. A certain number of vacant cationic positions should thus be inserted in the model to account for the actual stoichiometry and this is bound to create more surface situations than actually considered in the 'per-

fect' model. Still, it is important to remark that it is extremely difficult to rationalize the distribution of cation vacancies in the aluminas lattice and, consequently, at the surface. For this reason until recently no one of the researchers who studied the OH spectrum of aluminas did actually consider the effects possibly caused in the OH spectrum by the presence of cation vacancies at the surface.

The model proposed by Peri started being considered insufficient in the seventies, basically not for structural reasons, but rather for chemical ones.

In those years, a vast catalytic literature flourished, that dealt with the activity of transition aluminas (mainly the $\gamma$- and $\eta$-$Al_2O_3$ phases) in several reactions like, for instance, o-$H_2$/p-$H_2$ conversion, $H_2/D_2$ exchange, H/D alkanes scrambling, etc. The site structure and activity postulated for the OH groups most likely involved in the catalytic reactions turned out to be hardly compatible with the OH geometry proposed by Peri's model.

Also adsorption studies on aluminas were abundant in those years and the reactivity observed for some surface OH species did not correspond to the reactivity (i.e., either acidity or basicity) suggested by Peri's model. As an example, consider the two OH species 1 and 2 of Table 1, characterized by the two highest $\nu_{OH}$ frequencies (3800 and 3775 $cm^{-1}$ respectively): being surrounded by four and three oxide ions respectively, they should possess a certain reactivity and a slightly basic character. What was being observed with various types of adsorbed species is that the highest $\nu_{OH}$ species (3800 $cm^{-1}$) is actually very little reactive (if at all) and does not exhibit basic character. Unlike that, the OH species absorbing at ca. 3775 $cm^{-1}$ was found to be by far the most reactive OH species on all aluminas.

The reactivity, or perturbability, of the OH band at ca. 3775 $cm^{-1}$ was observed and successively confirmed, with respect to both weak bases like CO [24] and strong bases like pyridine [25]. A very selective reactivity was observed also with respect to mild acids like $CO_2$ [26] and was later confirmed with respect to strong acids [27,28].

Besides the plain number of nearest oxide neighbors, other parameters started then being considered as responsible for the variety of OH species in the spectrum of transition aluminas.

### *3.2. The role of OH coordination number. Tsyganenko's model*

Tsyganenko and Filimonov [21] examined the $\nu_{OH}$ vibrations of a very large number of metal oxides, including transition aluminas, grouped according to the crystal structure. Considering the most probable terminations of the crystallites and the geometry of the OH groups in these terminations, they came to the conclusion that the number of nearest neighbors has a negligible effect (if any) on the frequency of the OH species, whereas the determining factor is the number of lattice metal atoms that the OH groups are attached to.

On the basis of the electronic characteristics of oxygen, there can be three types of OH groups, termed OH groups of type I, II and III respectively, differing for the coordination number of the OH group. The three types of hydroxyls are shown in Scheme 3.

Since the formation of $M$–O coordinative bonds results in a lowering of the O–H stretching force constant, and thus of the relevant $\nu_{OH}$ frequency, the position of OH species of type I (terminal), type II (bridged) and type III (tribridged) should be observed in the spectrum in

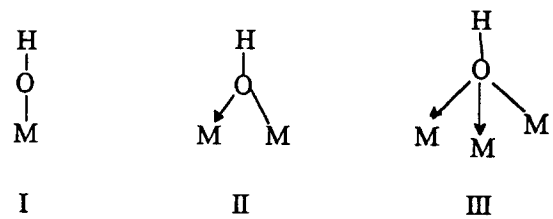


Scheme 3. Three types of hydroxyl groups are possible at the surface of transition aluminas, and of other metal oxides (from Ref. [21]).

the order of decreasing wavenumbers. The assignment of $\nu_{OH}$ bands proposed by Tsyganenko and Filimonov [21] is reported in the fourth column of Table 1.

This model has proved so far to be valid for the interpretation of the OH spectral pattern of many different metal oxide systems. For this reason, Tsyganenko and Filimonov's approach is still being adopted in these days for the identification and differentiation of OH species at the surface of systems either not studied before or for which different preparations lead to different crystal phases and/or to different crystal terminations.

In spite of the schematic graphical representation given in Scheme 3, in Tsyganenko's model all $M$–O bonds for the various OH species are considered as equivalent. For this reason, in the case of (spinel) transition aluminas the OH spectrum was expected to be grossly made up of three main absorption domains, centered around ca. 3790, ca. 3740 and ca. 3700 $cm^{-1}$. In fact, crystals termination along the most probable (111) and (100) planes, whose schematic lay-out proposed by Tsyganenko and Filimonov [21] is shown in Fig. 5, implies that all three types of OH groups are likely to be present at the surface of transition aluminas.

The fact that some of the OH bands of alumina are actually split in two (or more) components (especially in the case of the OH species I and II) was ascribed by Tsyganenko to

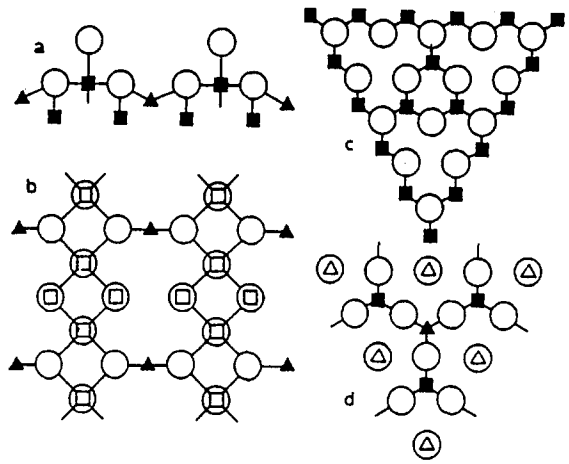


Fig. 5. Model of the fully hydroxylated surface of $\gamma$-$Al_2O_3$. (a) Cross-section and (b) plan view of the (100) plane. (c) and (d) are two possible variants of the surface for the (111) plane. All OH lie in the same plane, while the metal atoms are under this plane. Symbols: O hydroxyl, Δ tetrahedrally and □ octahedrally coordinated Al atoms (from Ref. [21]b).

the fact that each type of OH groups may differ for the coordination number of the surrounding metal atoms. In fact, it was recognized that both $Al^{IV}$ and $Al^{VI}$ ions can be exposed at the surface, if cleavage of the spinel lattice is carried out perpendicular to the [111] crystallographic direction.

This was the first time that the double coordination of Al ions in spinel aluminas was taken into account and was considered partly responsible (i.e., producing some kind of second-order effect) for the multiplicity of OH bands observed in the spectra of transition aluminas.

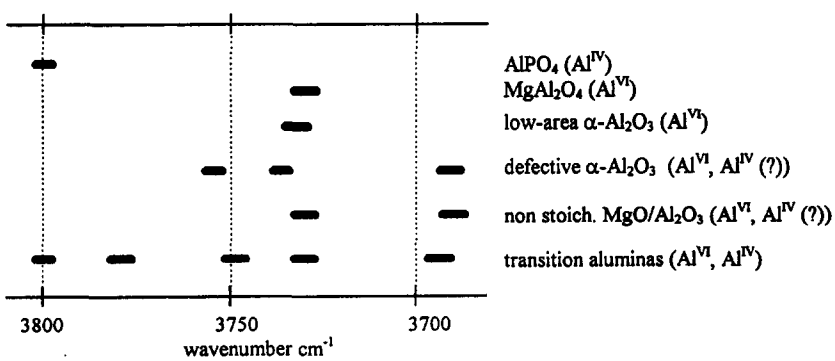


Scheme 4. Schematic distribution of $\nu_{OH}$ bands in some Al oxidic systems (from Ref. [31].)

### 3.3. The role of cations coordination number

Other research groups were active in the same years on the spectral properties of the various Al-containing oxidic systems and in particular on the complex spectra of their surface OH groups. For instance, Morterra and co-workers considered the coordination of the Al cation(s), rather than the coordination of the OH group, as the most important factor in determining the $\nu_{OH}$ frequency [29–31]. According to that approach, that did not consider the actual crystallographic termination of transition aluminas and of other Al-containing systems, the assignment of the various OH species of aluminas could be made only in very general terms, by comparing the OH spectra of different Al oxides. This 'overall' assignment of OH groups, based only on the coordination of the cations, is reported in Scheme 4.

The presence of the sole tetrahedral coordination for Al ions, like in the case of $AlPO_4$ [32], is observed to bring about the appearance of Al–OH bands only in the 3800–3770 $cm^{-1}$ interval, whereas the presence of the sole octahedral coordination for Al ions, like in the case of $\alpha$-$Al_2O_3$ and of Mg spinel [29,30], brings about the appearance of Al–OH bands (up to two bands) only at frequencies around 3730 $cm^{-1}$ and below. The presence, on transition aluminas, of more complex spectra and more numerous components was then considered as the consequence of the simultaneous presence, in these systems, of the double coordination for surface Al ions.

This gross assignment of OH bands, based on the coordination of the surface Al ions (it is schematically reproduced in Scheme 4), certainly did not explain all the spectral features of the OH pattern of transition aluminas. Still, that schematic distribution pattern has been confirmed by other more recent data relative to $\alpha$-$Al_2O_3$ (see Refs. [11,33] and see also spectrum e of Fig. 3), to various regular spinels [23,34], and to crystalline and amorphous AlOOH (see Refs. [5,14] and see also spectrum a in Fig. 3): these are all systems in which only $Al^{VI}$ ions are expected to be present.

### 3.4. The role of the net charge at OH. Knözinger's model

Moving from the inadequate description of Peri's model [22], from the relationship between OH coordination and OH frequency first proposed by Tsyganenko and Filimonov [21], and from the existence of a correlation between cations coordination and OH frequencies [29], in 1978 Knözinger and Ratnasamy [35] proposed a very detailed model for the surface of transition aluminas. That model remains, up to now, the most complete approach to the understanding of the complex OH spectrum exhibited by transition aluminas.

The basic assumptions of Knözinger's model are: (i) the termination of aluminas crystallites occurs along a limited number of low-index crystal planes and namely the (111), (110) and (100) planes. Note that this hypothesis, based mainly on the ions density of the various planes and on the likelihood of low index faces, tends to be largely confirmed by more recent HRTEM data [6], at least for what concerns the 'top' termination of the tiny flat particles constituting the most usual morphology of transition aluminas; (ii) the uppermost layer of the exposed crystal planes reproduces the anion and cation array typical of the bulk, i.e., no reconstruction and ion migration phenomena occur during the dehydration process at temperatures as high as ca. 1100 K; (iii) the frequency of OH species is imposed by the net electrical charge at the OH group. The net charge is determined by the coordination number of both the OH group (as in the scheme given by Tsyganenko and Filimonov [21]) and of the Al cation(s) involved (as in the scheme by Zecchina et al. [31]); in fact the net charge is 'obtained as the sum of the negative charge of the anion and the sum of the strengths of the electrostatic bonds ( = cation charge divided by coordination number) to the anion from adjacent cations' [35].

Based on these considerations, Knözinger singled out, within the three crystal planes, nine possible OH configurations that, neglecting possible differences of relative orientation of the OH group with respect to the cation(s), reduced to the five configurations reported in Scheme 5.

The average $\nu_{OH}$ frequency ascribed to each of the five configurations is indicated, together with the net charge at the OH group, in Scheme 5. This assignment is also reported in the fifth column of Table 1.

With the net charge, that changes the O–H stretching frequency, also the acidity (basicity) of the hydroxyl groups is expected to change: the lower the spectral position, the higher the acidity of the group. In this respect, the highest $\nu_{OH}$ band (ca. 3800 $cm^{-1}$, type $I_b$) should possess highest basicity, and the lowest $\nu_{OH}$ band (ca. 3690 $cm^{-1}$, type III) should possess highest acidity. This correlation turns out to be only marginally respected: in fact, a high $\nu_{OH}$ frequency does indeed correspond to a higher basicity, but this turns out to be far more true for the 3775 $cm^{-1}$ band (type $I_a$) than for the 3800 $cm^{-1}$ one (type $I_b$). Moreover, no particularly strong acidity is normally observed for low $\nu_{OH}$ bands (e.g., for type III OH groups).

The major merit of Knözinger's model is that, starting from a large and realistic number of possible crystal terminations, it reaches a limited number of possible OH configurations. This number virtually coincides with the number of OH components actually observed in the spectrum of all crystalline transition aluminas, provided that only $\nu_{OH}$ modes at $\tilde{\nu}$ > ca. 3680 $cm^{-1}$ are ascribed to OH species free from H-bonding. For this reason the OH scheme proposed by Knözinger is still being prevalently adopted in these days (e.g., see [19,36,37], whenever the adsorptive properties of aluminas need to be somehow related to surface OH species and to the surface dehydration process.

It is also interesting to note that: (i) Knözinger's model is fully consistent with Tsyganenko's assignment (e.g., compare columns 4 and 5 in Table 1), in that the coordination of the OH groups remains in the two treatments the main parameter in determining the $\nu_{OH}$ spectral position, whereas the coordination of the adjoining cation(s) represents a sort of fine structure factor; (ii) the description given by Knözinger is only partly in agreement with that proposed by those authors [31] who assumed the coordination of cation(s) as the main parameter: the

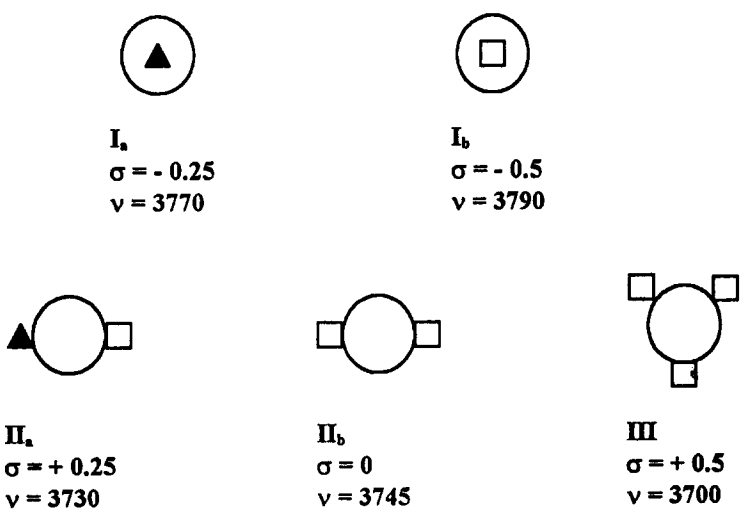


Scheme 5. Five possible OH configurations at the surface of spinel aluminas (from Ref. [35]). (Symbols: large circles represent OH groups; ▲ and □ represent tetrahedrally and octahedrally coordinated Al cations respectively; $\sigma$ stands for the net OH charge; $\nu$ stands for the average $\nu_{OH}$ frequency).

assignment of OH groups of type $I_a$ (terminal, purely tetrahedral), $II_b$ (bridged, purely octahedral) and III (tri-bridged, mainly or exclusively octahedral) is the same in the two models, whereas it is in contrast for the other two species. In particular, the species termed $II_b$ by Knözinger (terminal, purely octahedral) is in contrast with the fact that no OH groups at $\tilde{\nu} > 3750$ cm$^{-1}$ are ever observed in systems in which only the octahedral coordination is possible for Al ions; (iii) Peri's model cannot be thought of as a special case 'contained' in the complete model proposed by Knözinger: in fact, the only termination considered by Peri, the (100) face, would yield in Knözinger's description the sole OH species of type III, whereas the distinctive parameter used by Peri to differentiate the five $\nu_{OH}$ frequencies would at most bring about a partial resolution or a broadening of the sole OH band of type III.

As all models, Knözinger's model is an ideal one and its weakness (a weakness that is certainly modest with respect to its merits) consists in the fact that:

(i) it does not consider reconstruction effects. The latter are most likely to occur during surface dehydration, especially at high temperatures, as demonstrated by:

– the appearance of surface-localized vibrational modes, dealt with in the previous section and their perturbation during adsorption–desorption processes,

– the virtually constant shape of the $\nu_{OH}$ spectrum of different aluminas, in spite of the fact that aluminas of different morphology [6] and of different order-disorder degree [19] can be obtained,

– the very small concentration of surface active sites obtained upon surface dehydroxylation, as pointed out by many catalysis and adsorption works (see the next section).

(ii) it does not consider the role possibly played by the presence, at the surface as well as in the bulk, of some of the cation vacancies imposed to the spinel structure by the $Al_2O_3$ stoichiometry.

(iii) it considers only regular surface terminations, as obtainable from ideal low-index crystal planes, whereas crystallographically defective configurations (i.e., stepped terminations and/or high index planes) should be quite frequent in high surface area mesoporous materials.

### 3.5. The possible role of cation vacancies

The role played by cation vacancies is very difficult to take into account, as there is no way to determine them directly. The possible surface occurrence of cation vacancies is one further parameter, besides OH and cations coordination, that has been considered in the most recent model for OH of aluminas, proposed by Busca et al. [11,23] and Della Gata et al. [34].

As a starting point, Busca's model uses the same general criteria successfully adopted by Knözinger and reported above, but the assignment is also based, on a phenomenological ground, on:

(i) the observation of the OH spectral patterns of several normal spinels (like $MgAl_2O_4$, $ZnAl_2O_4$), inverse spinels (like $NiAl_2O_4$) and defective spinels (like the transition phase $\delta$-$Al_2O_3$);

(ii) the spectral characteristics of metal-hydroxy complexes having non-H-bonded OH groups with different coordination numbers.

The conclusions reached, that are schematically reported also in the last column of Table 1, reassign the various OH species of aluminas as reported in Scheme 6.

In particular, Busca's proposal modifies somewhat the assignment previously proposed by Knözinger in the sense that:

(i) we must observe a large difference of $\nu_{OH}$ position and not just a small difference, if the OH is bound to $Al^{IV}$ or to $Al^{VI}$ ions. This is particularly evident in the case of the two possible terminal OH groups (see a and c in Scheme 6), for which the $\Delta\nu_{OH}$ is as large as ca. 60 cm$^{-1}$. (In Knözinger's treatment, the $\Delta\nu_{OH}$ between OH groups of type $I_a$ and $I_b$ is only ca. 20 cm$^{-1}$). Incidentally, this description goes

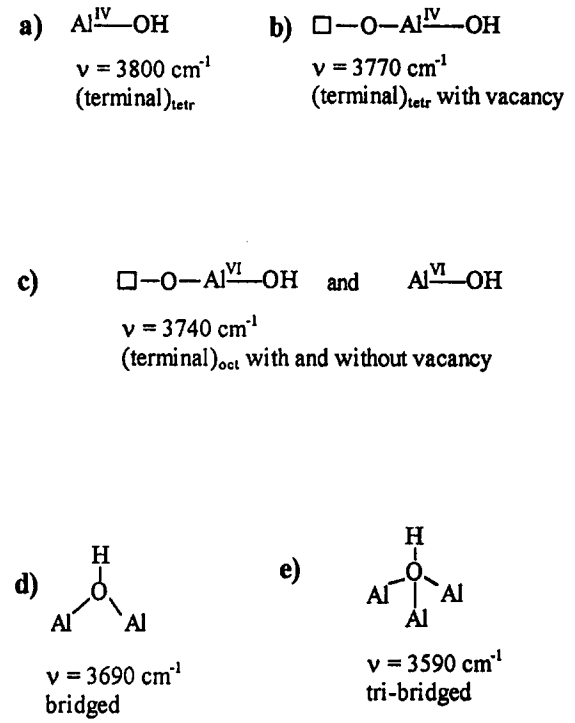


Scheme 6. Possible OH structures, and $\upsilon$OH frequencies, at the surface of defective spinel transition aluminas. (Symbols: □ stands for a cation vacancy; $\upsilon$ stands for the average $\nu_{OH}$ frequency).

back to the interpretation suggested by those authors [31], who claimed that the coordination of the cation is the prevailing factor in deciding the $\nu_{OH}$ frequency.

(ii) the free OH bands are distributed over a much wider spectral range than considered before. In particular, the OH species at 3700–3670 $cm^{-1}$ (type III in Knözinger's scheme), either resolved in two components or not, is ascribed to bi-bridging groups, whereas the band at ca. 3590 $cm^{-1}$ (previously assigned by all authors to H-bonded OH) is ascribed to tri-bridging OH, in agreement with data from hydroxy complexes [38].

(iii) the presence at the surface of cation vacancies is an important factor in determining the multiplicity of OH bands observed on transition aluminas. In particular, the resolution of the high $\nu_{OH}$ $Al^{IV}$-OH band in two components (3800 and 3775 $cm^{-1}$) is due to the presence of a cation vacancy in the coordination sphere of the $Al^{IV}$ responsible for the lower $\nu$ component (see b in Scheme 6). The vacancy determines a higher basicity of the oxide ions surrounding the Al ion and this affects (i.e., lowers) the $\nu_{OH}$ frequency.

The changes introduced by Busca's model into the assignment proposed by Knözinger are not dramatic, but are not small either. Both models contain a fair number of simplifications and of a priori assumptions and, at the same time, both models fit an appreciable number of (different) experimental observations. As a consequence, it is difficult to decide which model is preferable; in fact, either of the two models has been used as a reference in recent works, dealing with some surface properties of aluminas with respect to which the nature and distribution of surface hydroxyls needed to be considered. In general, in recent works Knözinger's model has been used more frequently (e.g., see [36,37]), probably in view of its being simpler and of its being there since a much longer time.

### *3.6. The possible role of defective crystal configurations*

Few last considerations remain to be done on the surface hydroxyls of aluminas and in particular on the OH species absorbing at ca. 3775 $cm^{-1}$. Its unique behavior has been anticipated in a previous section and deserves here some further comment.

(i) The band is present only on (all) transition aluminas, whereas it is totally absent on boehmite (see Ref. [14] and see also curve a in Fig. 3) and on well crystallized $\alpha$-$Al_2O_3$ (see Ref. [5,11,14,29] and see also curve e in Fig. 3). It is thus certainly ascribable to OH groups involving in their coordination sphere $Al^{IV}$ ions and this is either in agreement or compatible with most of the OH models proposed. What the various models proposed do not explain is why the OH band at ca. 3775 $cm^{-1}$ is *by far* the sharpest and the most reactive OH species at the surface of aluminas.

Actually, Busca's model does predict a different activity for this OH species (□-$Al^{IV}$–OH) with respect to its high frequency partner ($Al^{IV}$–OH; $\nu = 3800\ cm^{-1}$), but the different activity should be expected to be a higher basicity. What is found in practice is, as mentioned before, that the 3775 $cm^{-1}$ OH species is more active in respect to all types of admolecules and participates more actively in all catalytic reactions involving OH groups.

It is our belief that the higher activity of the 3775 $cm^{-1}$ species reflects mainly a higher accessibility of the OH species to all types of surface probes and this should reflect the possible presence of the OH group in particularly exposed zones of the surface. For this reason, in a recent paper Morterra et al. [19] have attributed the OH band at 3775 $cm^{-1}$ to $Al^{IV}$–OH groups present in portions of the surface belonging to crystallographically defective configurations. The latter are expected to be quite frequent in porous systems of high surface area and poor crystallinity; it is here recalled that Soled [4] showed how the surface area of $\gamma$- and $\eta$-$Al_2O_3$ must be high for structural reasons (and, in fact, it is normally as high as 200–250 $m^2g^{-1}$).

None of the models discussed so far indicates a special accessibility for the OH species responsible for the 3775 $cm^{-1}$ band. This is possibly so because all models discuss the surface of spinel aluminas only in terms of regular crystal plane terminations (the 'top' termination of particles) and do not consider the large incidence of structural defects in high area porous materials (the 'side' terminations of particles). The 3775 $cm^{-1}$ OH band has been considered, in all models proposed, as due to a 'regular' OH species, whereas it is probably not.

(ii) The unique nature of the OH band at 3775 $cm^{-1}$ is demonstrated also by its lability.

It was previously reported by Zecchina et al. [31] and it is here confirmed by the spectra in Fig. 6A, that on low-temperature transition aluminas (and especially on $\eta$-$al_2O_3$) the thermal elimination of the OH band at 3775 $cm^{-1}$ (at

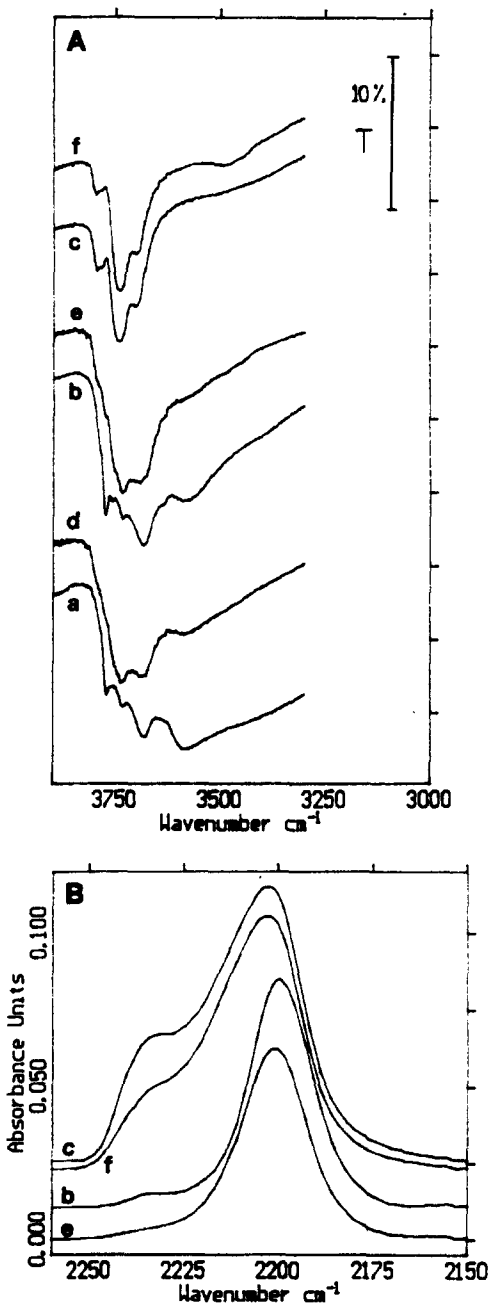


Fig. 6. Section A: the OH spectral pattern of an $\eta$-$Al_2O_3$ sample treated in various conditions. (a–c): the starting ("virgin") sample, activated at 673, 773, and 1023 K respectively. (d–f): after activation at 1123 K (almost complete dehydroxylation), the sample was rehydrated at 300 K, and further activated 673, 773, and 1023 K respectively. Section B: the spectrum of CO adsorbed at ambient temperature on $\eta$-$Al_2O_3$ isolated in some of the activation steps presented in section A.

temperatures as high as ca. 1100 K) is a mostly irreversible one.

Rehydration at ambient temperature of the virtually fully dehydrated alumina, followed by a second dehydration run, yields an OH pattern in which the relative intensities of the various OH species are altered and, in particular, the band at 3775 $cm^{-1}$ is very scarce and, sometimes, virtually absent. Only if the rehydration process is carried out with water vapor at temperatures as high as 670 K, in a sort of hydrothermal process [23,28], does the band at 3775 $cm^{-1}$ recover most of its original intensity [31]. This indicates that, during the high temperature dehydration of aluminas, reconstruction effects are operative and that the most defective configurations (i.e., those yielding the most reactive surface sites) tend to be annihilated.

A forthcoming section, devoted to surface acidity and to the interaction of aluminas with CO, will discuss in some more detail what is here anticipated by Fig. 6B: in low-temperature transition aluminas there is a direct correlation between the intensity of the OH band at 3775 $cm^{-1}$, as obtainable in a medium-high dehydration stage and the intensity of the strongest CO adspecies ($\nu_{CO}$ ca. 2240 $cm^{-1}$, ascribed to CO chemisorption onto the most defective $Al^{IV}_{cus}$ sites), as obtainable upon CO uptake on the aluminas after activation at the same temperatures. This agrees with the hypothesis that the OH band at 3775 $cm^{-1}$ is mainly due to crystallographically defective configurations at which dehydration creates the most active sites. During activation at high temperatures, some (or most) of the defective configurations are annihilated by surface reconstruction effects, so that both the $\nu_{OH}$ band at ca. 3775 $cm^{-1}$ and the $\nu_{CO}$ band at ca. 2240 $cm^{-1}$ tend to be absent.

The interpretation here proposed for the OH band at 3775 $cm^{-1}$ is confirmed by the behavior of the high-temperature transition aluminas. As mentioned in the introduction section, structurally these aluminas are still defective spinel systems, but characterized by higher crystalline order, larger crystallites and more regular (i.e., sharper) terminations of the particles. In the OH spectral region (see, for instance, curve d of Fig. 3), the higher order of the high-temperature transition aluminas is reflected by a clear splitting of the OH bands of type II (two components are resolved at ca. 3745 and ca. 3730 $cm^{-1}$) and sometimes also of the OH bands of type III (two components are often resolved at ca. 3710 and ca. 3680 $cm^{-1}$ [37]). But the OH species at 3775 $cm^{-1}$, that was tentatively ascribed to $Al^{IV}$-OH groups in exposed and/or defective crystallographic configurations, is either very weak (as it is in curve d of Fig. 3) or totally missing [18,19,36].

Also the adsorption of CO confirms this datum: on $\delta$-$Al_2O_3$ [18] and on $\theta$-$Al_2O_3$ [19] a band of strongly adsorbed CO, located at $\nu >$ 2230 $cm^{-1}$, is either missing or very weak, as will be reported in more detail in a following section.

## 4. The basicity of aluminas

An entire chapter of this issue is devoted to the basicity of catalytic systems and to its determination with spectroscopic methods. Consequently, we will limit ourselves to very few preliminary considerations on the basicity of the family of oxides we are here dealing with.

The surface basicity of transition aluminas is quite low: in fact, $Al_2O_3$-based catalysts are fairly important, on a catalytic and on a conventional chemical ground, for their acidity rather than for their basicity. As a consequence, whenever a basic catalyst or catalyst support is needed, either other oxides are resorted to or aluminas are doped with variable amounts of basic elements [39–41].

For a long time the surface basicity of oxides has been tested by the gas-solid adsorption of $CO_2$. From very recent applications, the adsorption of $CO_2$ seems to be still the routine way to evaluate the basicity of aluminas and of its changes with surface chemical modifications [40,42].

It is known that the ambient temperature adsorption of $CO_2$ onto ionic oxides leads to two types of interaction and yields two families of adsorbed species: (i) there is a linear form of cation-coordinated $CO_2$, that has been sometimes improperly termed physisorbed $CO_2$. This species, that is often correlated to some adsorbed species of the second family [43], reveals coordinative vacancies on cations at the surface (Lewis acidic sites). This type of $CO_2$ adsorption will be dealt with in the next section, devoted to surface acidity of aluminas; (ii) there are various types of bent $CO_2$ adspecies (i.e., surface species in which $CO_2$ looses its linear shape). In these species, that are usually termed carbonate-like species, the interaction occurs either at surface basic sites or at surface acid-base pair sites.

The various carbonate-like species are recognizable, by comparison with numerous inorganic and coordination compounds, on the basis of the number and relative position of their (several) vibrational modes [44]. A systematic description of the various carbonate-like species formed on metal oxides has been done by Busca and Lorenzelli [45]; also correlation tables of the type reported in Scheme 7 are available in the literature so that, nowadays, the assignment of carbonate-like species at the surface of metal oxides is very seldom controversial.

The adsorption of $CO_2$ onto transition aluminas started being studied since the earliest days

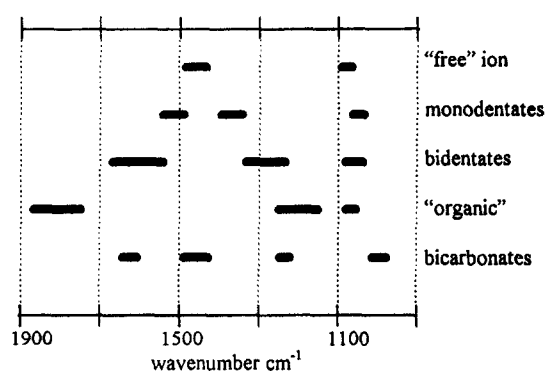


Scheme 7. Schematic representation of the band positions of carbonate-like species at the surface of metal oxides (from Ref. [46]).

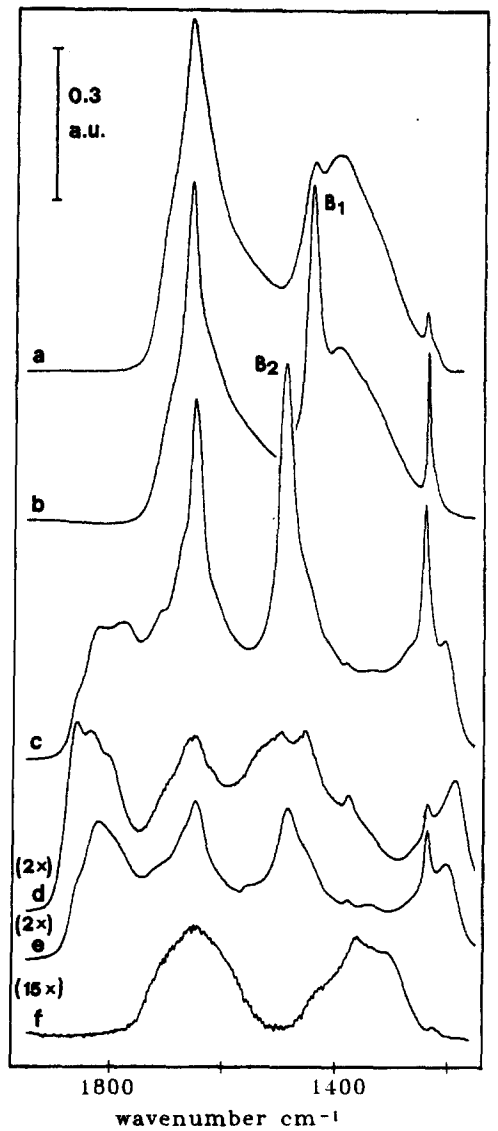


Fig. 7. IR absorbance spectra of $CO_2$ adsorbed, in a bent form, on various Al oxidic systems. (a): $\gamma$-AlOOH, activated at 300 K. (b–d): $\gamma$-$Al_2O_3$, activated at 300, 773, and 1023 K. (e): $\theta$-$Al_2O_3$, activated at 773 K. (f): $\alpha$-$Al_2O_3$, activated at 1023 K. (Some of the spectra underwent an ordinate scale expansion, as reported in the figure).

of IR spectroscopy of adsorbed species (e.g., see Ref. [20], p. 74–84, [26,47,48]), whereas it is more recent the study of the interaction of $CO_2$ with $\alpha$-$Al_2O_3$ [49] and with Al hydrates [14].

Fig. 7 reports the IR spectra of carbonate-like species formed at the surface of various Al oxidic systems, isolated in some significant

stages of the surface dehydration process.

The overall spectral features of $CO_2$ adsorbed at ambient temperature on Al oxides can be summarized as follows.

(i) On the $\gamma$-AlOOH phase, activated at low temperatures (300–400 K), there is the abundant formation of monodentate carbonates (see curve a of Fig. 7; $\nu_{CO}$ modes at ca. 1600 and ca. 1400 $cm^{-1}$) and of very small amounts of bicarbonates. The spectrum of carbonates at the surface of the Al hydrate phase gradually changes after activation at higher temperatures, but this was shown to be mainly due to the onset of a gradual surface phase transformation towards transition $Al_2O_3$ phases [14].

(ii) On the low-temperature transition alumina phases (spectra b, c and d in Fig. 7 refer to $\gamma$-$Al_2O_3$; the behavior of $\eta$-$Al_2O_3$ is much the same [43]), the situation is more complex and quite different from that of Al hydrates. In fact:

- After activation at relatively low temperatures, there is mainly the formation of a family of bicarbonates (previously termed $B_1$ [43]), characterized by strong $\nu_{CO}$ bands at ca. 1650 and ca. 1440 $cm^{-1}$, by a $\delta_{OH}$ band at ca. 1230 $cm^{-1}$ (see spectrum b of Fig. 7) and by a $\nu_{OH}$ band at ca. 3618 $cm^{-1}$.- After activation at temperatures in the interval 573–973 K, i.e., when the surface hydroxyls are still abundant and become basically free from H-bonding, the bicarbonate species termed $B_1$ declines while another bicarbonate species, termed $B_2$ [43] forms (see spectrum c of Fig. 7). The formation of $B_2$ happens mostly at the expense of the basic ('reactive') OH species at 3775 $cm^{-1}$ ($I_a$) and of part of the OH species at 3690 $cm^{-1}$ (III), that was supposed to have acidic character [35]. The bicarbonate species $B_2$ is characterized by minor frequency differences in most of the observable bands (e.g., the $\nu_{OH}$ and $\delta_{OH}$ modes) and by a fairly different position for the symmetric $\nu_{OCO}$ mode, that is now located at ca. 1480 $cm^{-1}$. (Note that transition aluminas are the only oxidic systems so far examined on which more than one surface bicarbonate species is formed).

Also a complex system of $\nu_{CO}$ bands centered at $\nu > 1700$ $cm^{-1}$ and at $\nu < 1200$ $cm^{-1}$, usually ascribed to bridging or 'organic-like' carbonates, starts to being formed [45].

- After activation at temperatures higher than 973 K (spectrum d of Fig. 7), when all bicarbonate species do not form any longer because virtually all of the proper hydroxyls have been eliminated, 'organic' carbonates become the predominant species, but also weak bands due to mono- and/or bidentate carbonates can be observed in the spectra; these bands were possibly present also on the materials dehydrated at lower temperatures, but their low intensity was obscured by the overwhelming intensity of abundant bicarbonate species.

As for the predominant species absorbing in the 1900–1700 $cm^{-1}$ and in 1200–1100 $cm^{-1}$ ranges (ascribed to bridging or 'organic-like' carbonates), an alternative assignment has been proposed by Busca and Lorenzelli [45]: the bands could be due to the vibrations of 'strongly perturbed $CO_2$ molecules', that interact via the carbon and the oxygen atoms with one or more (up to three) cus surface cations. These strongly perturbed $CO_2$ species are expected to posses low stability: as within the complex of bands at 1900–1700 and 1200–1100 $cm^{-1}$ there are some minor components (approximately 1/5 of the total integrated absorbance) that are quite labile with evacuation. It is possible that some complexes do actually exist in which the $CO_2$ adspecies interacts with a bent configuration only with cus cations, but it is our belief that the major component of the bands is due to strongly held bridging structures of the 'organic-like' type, in which the adsorbed $CO_2$ molecule shields at the same time a cus cation and a cus anion.

(iii) On the high-temperature transition $Al_2O_3$ phases, the situation is very similar to that just described for the low-temperature phases. The only remarkable difference (described by curve e of Fig. 7, to be compared to curve c [41]) is that at intermediate stages of dehydration the intensity of the bands due to $B_2$ bicarbonates is

much lower, whereas the relative intensity of bands due to bridging structures is higher. This is consistent with the formation of $B_2$ bicarbonates mostly at the expense of the OH band at 3775 $cm^{-1}$, whose intensity on high-temperature transition aluminas was shown in a previous section to be scarce and, sometimes, virtually zero.

(iv) On the $\alpha$-$Al_2O_3$ phase, the situation becomes different again and definitely simpler (see, for instance, trace f in Fig. 7). In medium-high dehydration stages, there is only the formation of (several) bidentate carbonates, whose bands are sharper and better resolved the higher the crystalline order achieved [49]. Only at low dehydration stages there is also the formation of monodentate carbonates, whereas the formation of bicarbonates is either zero (on well crystallized $\alpha$-$Al_2O_3$ preparations) or is very weak and of the sole $B_1$ type on poorly crystallized $\alpha$-$Al_2O_3$ preparations [49].

This quick overview of the bent $CO_2$ species formed, upon $CO_2$ uptake, on the various Al oxidic systems allows us to conclude that: (i) the formation of bicarbonates, that on aluminas as on other oxides tend to assume a bridging configuration [26,43,45], is peculiar of the systems in which the surface can expose $Al^{IV}$ ions and/or $Al^{IV}$–OH terminal groups (i.e., it is typical of transition aluminas). On Al oxidic systems that present the sole $Al^{VI}$ coordination, bicarbonates do not form, possibly because no OH groups of the proper basicity are present. (The small amount of bicarbonates formed on $\gamma$-AlOOH [14] and on some poorly crystallized $\alpha$-$Al_2O_3$ preparations [49] must be ascribed to the presence of a few Al ions bearing a (quasi-)tetrahedral coordination); (ii) on highly dehydrated systems that can expose $Al^{IV}$ ions, the counterpart of bicarbonates are carbonate structures bridging across two adjacent Al coordination spheres (the species most often termed 'organic-like' carbonates). On Al oxidic systems that present the sole $Al^{VI}$ coordination, organic carbonates do not form; (iii) on transition aluminas, the formation of monodentate and bidentate carbonates is very scarce, possibly because other stronger $CO_2$ adspecies are favored. Unlike that, on Al oxidic systems that present the sole $Al^{VI}$ coordination, monodentate and bidentate carbonates are the only carbonate-like species formed.

It is thus deduced that the octahedral coordination of Al ions can give to (some) surface $O_{cus}$ ions in their coordination sphere sufficient basicity, whereas $Al^{IV}$ ions cannot.

It is of some interest to compare the spectral results on the basicity of Al oxides also with some quantitative data [39,40,42,43].

(i) On transition aluminas, the amount of $CO_2$ that adsorbs so strongly as to resist to evacuation at ambient temperature, i.e., most of the carbonate-like species, varies with sample activation temperature between ca. 0.3 molecules $CO_2$ per $nm^2$ (when the hydroxylation is still quite high and bicarbonates predominate) and ca. 0.6 molecules $CO_2$ per $nm^2$ (when the surface is almost bare and bridging structures dominate).

(ii) In the case of well crystallized $\alpha$-$Al_2O_3$, the adsorbed amounts depend much less (if at all) on the surface dehydration and are approximately twice as large as on transition aluminas.

If one considers that 1 $nm^2$ of one of the spinel crystal faces most favorably exposed contains ca. 14–18 anions and roughly 2/3 that many cations [21,35], the data on $CO_2$ uptake clearly confirm that the basicity of transition aluminas is, in general, quite low, though not negligibly low (some approximate calculations and sites hypotheses were reported for $\eta$-$Al_2O_3$ in Ref. [43]).

Assuming that one $CO_2$ molecule adsorbed in the form of (any type of) carbonate-like species occupies two average anion positions on the spinel alumina surface. It is guessed that bent-$CO_2$ uptake probes at most ca. 10% of the surface. This is a very crude estimation of the surface coverage achieved, but it indicates that the rough figure (ca. 10%), a figure that is quite small with respect to the theoretical amount of coordinative vacancies created upon dehydra-

tion, is still about one order of magnitude larger than the number of catalytically active centers towards which $CO_2$ was reported long ago to be a selective poison [50].

## 5. The acidity of aluminas

As for the basicity of catalytic systems, also the acidity of catalytic systems and its determination with spectroscopic methods is the subject of an entire chapter of this issue. Therefore, only few preliminary considerations will be introduced in this section.

The surface acidity of polydispersed solid systems is a very important property and its determination, though often complex, is of primary technological importance. Many different techniques are normally adopted to test surface acidity (e.g., see [51,52] and references therein), but the results obtained are sometimes ambiguous and/or contradictory. In general terms, it can be suggested that: whenever, for the determination of the acidity, (quantitative) analytical techniques based on the adsorption of selected probe molecules are resorted to, these techniques should be complemented with IR measurements. In fact, only the spectroscopic observation of the type and number of adsorbed species formed and/or of the possible reaction products, may render the analytical determinations completely meaningful.

In the case of transition aluminas, whose surface acidity is by far the most important feature, the IR technique has been used quite extensively and a great variety of adsorbing probe molecules has been tried. Merits and limits of the various IR-adsorption procedures adopted have been reviewed by Knözinger some years ago [53] and to the best of our knowledge no more recent reviews have been produced.

In the present contribution, devoted to surface chemistry and structure of catalytic aluminas, we shall not report the results obtained by so many authors, who used the spectroscopic approach to describe the adsorption of so many different adsorbates. Instead, we will concentrate mainly on the adsorption of relatively few adsorbed species that, in our opinion, have yielded in the years clear information on the nature (and possibly on the amount) of acidic centers at the surface of Al oxides.

### *5.1. The adsorption of strong bases*

Strong bases, as adsorbates, should in principle be suitable probes for the evaluation of the overall acidity of oxides, as well as to distinguish between protonic (Brønsted) acidity and aprotic (Lewis) acidity.

*5.1.1.1. Amines.* Among strong bases, a large variety of amines has been used. The conclusion, reported by Knözinger in his review [53], is that it is difficult to gain from the adsorption of amines unambiguous indications on the chemical nature and on the number of aluminas active sites. This is mainly due to the fact that the adsorbed amount of an amine, on transition aluminas as well as on other oxides, depends primarily on its molecular cross-sectional area and not on its basicity [54]. Moreover, amines can undergo quite easily various surface reactions, especially if a desorption process is carried out at relatively elevated temperatures.

*5.1.1.2. Ammonia.* The adsorption of ammonia as a probe for the surface acidity of aluminas has been used by several investigators (e.g., see [54–58]) and is still being used in these days [40,52]. In general, microcalorimetric and TPD determinations of ammonia adsorption are routinely used to evaluate the (total) acidity of a catalyst, but in our opinion the use of this base does not give the best results.

The advantage of using ammonia as an adsorbate to test acidic centers is twofold: (i) due to the high basicity and the small molecular size, ammonia reveals as many acidic sites as possible. In this way, the total concentration of acid centers at the surface of transition aluminas

is usually reported to be approximately four-to-five times larger than the total concentration of basic sites [40,52]; (ii) the IR spectra of adsorbed ammonia can clearly differentiate Lewis and Brønsted acidity. In this way, some authors, but not all authors, have shown that some OH groups at the surface of transition aluminas possess sufficient acidity to yield adsorbed $NH_4^+$ species (adsorbed $NH_4^+$ is characterized by a strong band at 1450–1480 $cm^{-1}$ and by weak bands at ca. 1700 and 1390 $cm^{-1}$ [40]).

The disadvantages of using ammonia as an adsorbate to test acidic centers are heavier than the advantages just described. They mainly depend on the fact that ammonia can interact in (at least) four different ways at the surface of an oxide and that IR spectroscopy is seldom sufficient in recognizing with accuracy which is which. In fact $NH_3$ can: (i) H-bond via one of the hydrogens to surface oxygens (either lattice oxygens or OH oxygens) or via the N lone pair to surface OH groups without the extraction of a proton; (ii) transfer a proton from acidic surface OH groups (Brønsted acid-base interaction), (iii) coordinate to cus surface cations (Lewis acid-base interaction). It is important to note that, if different families of Lewis acid sites exist at the surface, as in the case of transition aluminas, the analytical bands of coordinated ammonia (ca. 1620 and ca. 1240 $cm^{-1}$ [40,44,53]) cannot differentiate them, whereas other bases like pyridine often do; (iv) dissociate on acid-base pair sites, yielding surface amido groups ($-NH_2$) and surface OH groups. This process, similar to that of rehydration brought about by water adsorption, yields new groups of high and different stability, whose spectroscopic features and surface concentrations are difficult to single out.

For these reasons, Knözinger in his review [53] reports that 'ammonia retention on aluminas cannot be an acceptable measure of surface acidity and can hardly be related to catalytic activity'.

*5.1.1.3. Pyridine.* The best results in the determination of the total acidity of aluminas (and, in general, of most metal oxides) can be obtained by the adsorption–desorption of pyridine (py) [53]. In fact py, although less basic than ammonia, is still a fairly hard base and can interact with sites of widely different acidity. Moreover, on non strongly basic systems, adsorbed py does not undergo surface reactions (at least up to quite high temperatures), so that py uptake data yield a better titration of surface acidity than all other strong bases.

Py can interact at the surface of oxidic systems in three ways: (i) the nitrogen lone pair can H-bond to surface weakly acidic OH groups, yielding a very weak perturbation of the adsorbed molecule (this type of interaction is symbolically referred to as [py-H]); (ii) if the

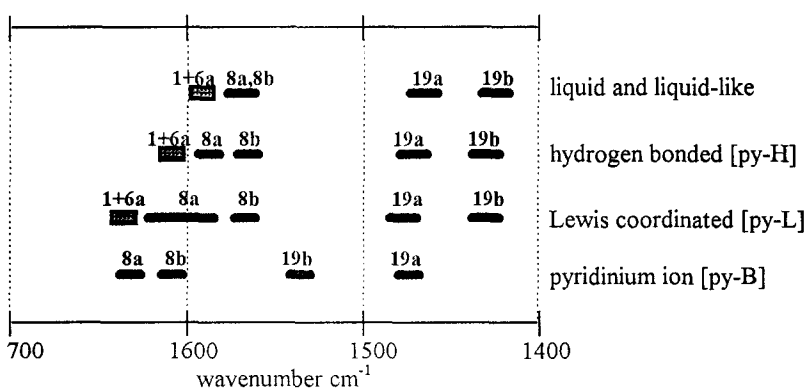


Scheme 8. Schematic representation of the spectral range of the 8a–8b, 19a–19b modes for some py-containing systems (No reference is made to the intensity ratio of the bands, nor to their breadth. The bars show the range of occurrence for the various vibrational modes. The difference between fundamental and combination modes is also indicated).

Brønsted acidity of a surface OH group is sufficiently high, a proton can be extracted to yield a pyridinium ion species ($pyH^+$; this type of interaction is symbolically referred to as [py-B]); (iii) the nitrogen lone pair can interact by $\sigma$-charge donation to surface cus cationic centers, acting as Lewis acid sites. (This type of interaction is symbolically referred to as [py-L]).

The ring vibrational modes 8a–8b and 19a–19b, according to the assignment of Kline and Turkevich [59], are the most sensitive vibrations of py with regard to the nature and strength of the adsorptive interaction. For this reason, inspection of the IR spectral region 1700–1400 $cm^{-1}$ of adsorbed py is routinely employed for the assessment of the surface acidity of metal oxides.

The large number of data available in the literature, concerning homogeneous and heterogeneous py compounds and complexes, allows to draw the schematic representation of the spectral range 1700–1400 $cm^{-1}$ and of the py vibrational modes therein, as shown by Scheme 8 [60].

Since Parry first proposed, in his pioneering work, the use of py as a suitable probe for surface acidity [61], several authors studied the interaction of py with various aluminas and the influence of pretreatment conditions on py uptake (e.g., see [62–65]). Most of these early works, confirmed also by more recent data on various Al oxides, indicate that only in the case of particular preparations and/or pretreatments does any Brønsted activity of py appear on aluminas [65]. In fact, for most pure alumina phases and for all pretreatment and/or reaction conditions, the $pyH^+$ species is not formed at a spectroscopically detectable level, due to the insufficient protonic acidity of all of the regular OH species of aluminas, dealt with in a previous section.

Most of the quoted authors recognized, at the surface of transition aluminas, the formation of weakly held [py-H] species and of strongly held [py-L] species, confirming the Lewis acidic nature of these systems.

*5.1.2. Py adsorption according to Knözinger*

In the early seventies, Knözinger and Stolz [66] first proposed a 'structural' interpretation of the Lewis acid-base interaction of py with transition aluminas ($\gamma$- and, mostly, $\delta$-$Al_2O_3$). Using increasing temperatures for py adsorption–desorption cycles, these authors isolated three different types of Lewis coordinated by species, characterized by having the analytical mode 8a centered respectively at 1614 $cm^{-1}$ (this species formed at 373 K), 1617 $cm^{-1}$ (species formed at 493 K) and 1624 $cm^{-1}$ (species formed at 573 K).

On the basis of the frequency of the 8a mode and of the resistance to thermal evacuation, the first two py adspecies were attributed to two 'outer' (weak) py Lewis complexes and the third py adspecies to an 'inner' (strong) py Lewis complex. The latter species (absorbing at 1624 $cm^{-1}$) was interpreted as being formed by transformation of the second adspecies (absorbing at 1617 $cm^{-1}$) as a consequence of an activated process that would lead the coordinated py molecule to a closer interaction with the relevant adsorbing sites.

The three coordinated py adspecies were observed by Knözinger and Stolz [66] to form in different amounts, following the activation temperature of the alumina, as described by Fig. 8.

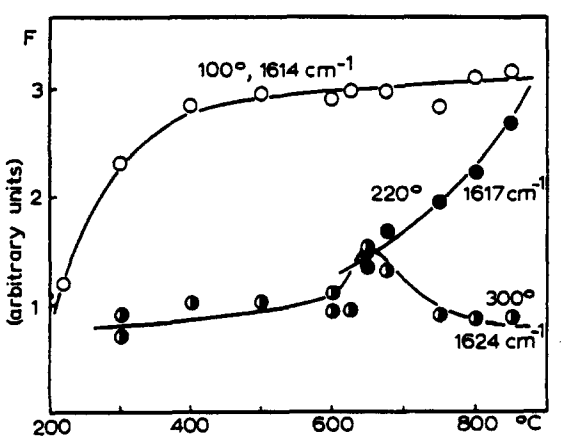


Fig. 8. Relative surface concentrations of py complexes, as a function of the activation temperature (°C) of the alumina (from Ref. [66]b).

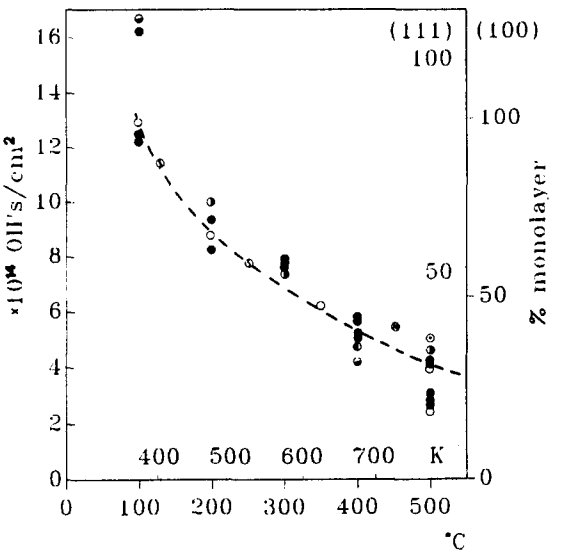


Fig. 9. Surface OH density of transition aluminas as a function of pretreatment temperature (from Ref. [35]).

On the basis of the py uptake trend of Fig. 8 and of the dehydroxylation trend of transition aluminas (the latter trend is shown in Fig. 9; the plot is 'averaged' from the data obtained by several authors, see [35] and references therein), the weakest py 'outer' complex was attributed by Knözinger and Stolz [66] to Lewis acidic centers constituted by single oxide vacancies, formed in the earliest stages of surface dehydration.

The stronger 'outer' complex was attributed to stronger Lewis acidic centers constituted by pair or triplet oxide vacancies, formed in more severe conditions of surface dehydration (i.e., within the temperature range corresponding to the final part of the plot in Fig. 9).

The strongest 'inner' complex was ascribed to the occurrence of a close coordinative interaction of py with the strongest Lewis acidic centers, constituted by triplet oxide vacancies.

Using still higher py adsorption–desorption temperatures (temperatures as high as 673 K), Knözinger and Stolz observed the elimination of the strong 'inner' complex, characterized by the 8a mode at 1624 $cm^{-1}$ and the formation of another intense band at 1634 $cm^{-1}$. The newly formed species was attributed initially to an even stronger py complex [66] and was successively ascribed to the transformation of (some of) the strongly coordinated 'inner' py complexes into an adsorbed $\alpha$-pyridone species [16,53]. The redox surface reaction would proceed, at the high temperature reached, onto acid–base pair sites, consisting of a cus Al ion and of a basic OH group, as described in Scheme 9.

The reactive site responsible for $\alpha$-pyridone formation was identified by Knözinger and Stolz as the 'X-site', defined by Fink [67] as responsible for the high catalytic activity of highly dehydrated aluminas (Fink's 'X-sites' are, for instance, the sites active towards $CO_2$ to yield bicarbonates and active in most of the alumina catalyzed reactions [50]). The site would consist of an exceptional configuration of rather low probability, containing three or more exposed aluminum ions or a doublet vacancy with an adjacent hydroxyl group [50]). A tentative model for the acid–base reactive sites termed Fink's 'X-sites' was later proposed by Knözinger et al. [16], together with his model for aluminas surface dehydration and is shown in Fig. 10.

According to Scheme 9, a basic OH group is actually needed for the $\alpha$-pyridone formation (as well as for the formation of bicarbonates) and it was identified with the 'reactive' OH absorbing at 3775 $cm^{-1}$. The surface concentration of the active 'X-sites' was evaluated to be in the order of $10^{13}$ $cm^{-2}$, i.e., of 0.1 sites per $nm^2$, corresponding to less than 1% of the surface of alumina these figures confirm the

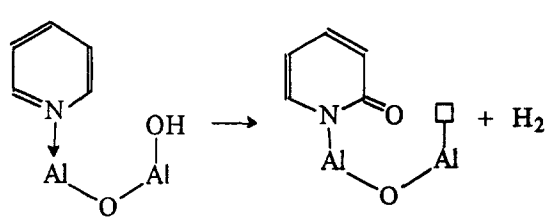


Scheme 9. The formation of adsorbed $\alpha$-pyridone from Lewis adsorbed py (from Ref. [16]). (The symbol □ stands for a coordinative vacancy, or anion vacancy).

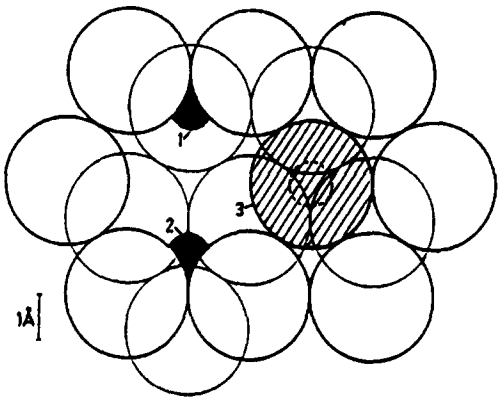


Fig. 10. Model acid-base pair site on a [111] face of $\eta$-$Al_2O_3$. 1:3-coordinate $Al^{3+}$ ion (equivalent to a species $Al^{IV}_{cus}$, as defined in the text); 2:5-coordinate $Al^{3+}$ ion (equivalent to a species $Al^{VI}_{cus}$, as defined in this text); 3: tetrahedral OH group (from Ref. [16]).

exceptional nature of the highly active sites and the anomalous nature of the $I_a$ OH groups absorbing at 3775 $cm^{-1}$.

The scheme proposed by Knözinger and Stolz for the Lewis acid–base interaction of py at the surface of transition aluminas [66] had the merit to evidence the multiplicity of [py-L] species formed on these systems (note that no other oxidic systems ever exhibited so many [py-L] species) and the different energy of interaction involved in the various adsorption processes.

The limit of Knözinger and Stolz's proposal consists in the failure to identify in the multiplicity of coordination states possible for surface Al ions the actual main origin of the multiplicity of [py-L] species formed on aluminas. Only few years after proposing this model for py adsorption, Knözinger produced his successful model for the surface of transition aluminas and for the interpretation of the OH spectrum [35]: at that point it became clear that the multiple coordination possible for Al ions bears also the main responsibility for the multiplicity of Lewis adsorbing sites present at the surface of dehydrated aluminas. The correlation between Al coordination state and [py-L] strength was first recognized by other authors (see next section).

*5.1.3. Py adsorption according to Morterra*

Consistent with the hypothesis previously formulated for the interpretation of the OH spectrum of transition aluminas [29,30], Morterra et al. [68] suggested that the coordination of the cus Al ions (acting as Lewis acid sites) is primarily responsible for the frequency exhibited by the analytical ring modes of adsorbed py and especially by the most sensitive mode 8a.

Fig. 11 reports segments of the spectra of py adsorbed on $\gamma$-AlOOH (a), $\gamma$-$Al_2O_3$ (b), $\theta$-$Al_2O_3$ (c) and $\alpha$-$Al_2O_3$ (d). The basis of the assignment proposed for the various py adspecies formed on transition aluminas consists in the observation that: (i) whenever Al ions possess the sole octahedral coordination (like in boehmite and corundum), there is the prevalent formation of virtually only one [py-L] species [14,69], whose 8a mode lies below 1600 $cm^{-1}$. This is more clearly true for well crystallized $\alpha$-$Al_2O_3$ (curves d of Fig. 11), whereas in the case of boehmite (curves a of Fig. 11) the presence of some quasi-tetrahedral Al ions leads to the appearance of weak [py-L] species also at $\nu > 1600$ $cm^{-1}$. Note that a weak band at $\nu >$ 1600 $cm^{-1}$ is always present in any event, due to the (1 + 6a) overtone, as described by Scheme 8. (ii) Unlike that, when also the tetrahedral coordination of Al ions is present, several [py-L] species form and the prevalent and more resistant of these species exhibit the 8a mode above 1600 $cm^{-1}$. The larger uncoordination degree achieved by $Al^{IV}_{cus}$ ions is responsible for a stronger charge release from the nitrogen lone pair and this brings about a larger upwards shift of the coordination-sensitive $A_1$ vibrational modes of [py-L].

This interpretation was confirmed by the spectra of py adsorbed on other systems, like $AlPO_4$ [32], highly dehydrated $SiO_2$ [70] and $MgO/SiO_2$ [71], in which the presence of tetrahedrally coordinated cus cations causes the 8a mode of adsorbed py to rise above ca. 1610 $cm^{-1}$.

Using an $\eta$-$Al_2O_3$ preparation dehydrated at

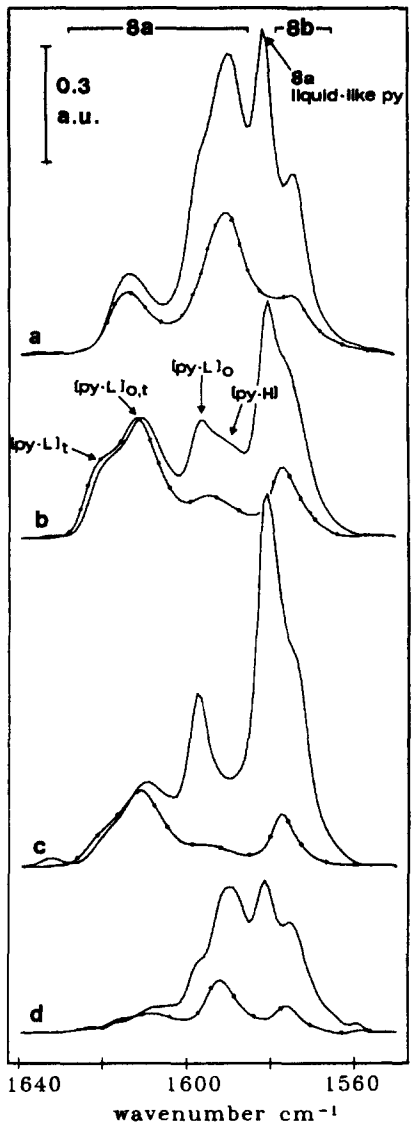


Fig. 11. The 1640–1550 $cm^{-1}$ spectral region (8a–8b modes) of py adsorbed at ambient temperature on some Al oxides ($P_{py} = 8$ Torr for the stronger spectra, and $10^{-2}$ Torr for the dotted-line weaker spectra). (a) $\gamma$-AlOOH activated at 300 K, (b) $\gamma$-$Al_2O_3$, activated at 773 K, (c) $\theta$-$Al_2O_3$, activated at 773 K, (d) $\alpha$-$Al_2O_3$, activated at 1023 K.

various temperatures in the 300–973 K interval, Morterra et al. [68] showed that: (i) at the surface of transition aluminas there can be up to four types of chemisorbed py. The weakest one, observable only in the presence of a py pressure, has the 8a mode at ca. 1590 $cm^{-1}$ and on the basis of its dependence on activation temperature can be ascribed to py H-bonded to some surface OH species ([py-H]). Another weakly held species is formed in small amounts, has the 8a mode at ca. 1598 $cm^{-1}$, is slightly more resistant to evacuation than the previous species and can be assigned to py Lewis coordinated to $Al^{VI}_{cus}$ ions ($[py\text{-}L]_o$). A third species, far more resistant to evacuation, has the 8a mode at 1610–1620 $cm^{-1}$ and was ascribed to py Lewis coordinated to coordinative vacancies shared by an $Al^{VI}$–$Al^{IV}$ cations pair ($[py\text{-}L]_{o,t}$). The fourth species, formed on alumina dehydrated at $T > 473$ K and definitely more resistant to evacuation than all other species, has the 8a mode at ca. 1625 $cm^{-1}$ and was ascribed to py Lewis coordinated to $Al^{IV}_{cus}$ sites ($[py\text{-}L]_t$). (ii) The $[py\text{-}L]_{o,t}$ species corresponds to the two 'outer' complexes of Knözinger's model. It is not a double species, but only a heterogeneous species, whose spectral features (i.e., the position of the 8a and 19b modes) depend on the temperature of activation of the alumina and on the temperature of evacuation of adsorbed py. This is the origin of an 8a mode of coordinated py centered at ca. 1614 $cm^{-1}$ in some cases and at ca. 1617 $cm^{-1}$ in others. (iii) The strongly held $[py\text{-}L]_t$ species corresponds to the 'inner' complex of Knözinger's model and is not formed at high temperature at the expense of any other py adspecies. Rather, its intensity strongly depends on the activation temperature of alumina in that the relevant $Al^{IV}_{cus}$ sites are the strongest Lewis acid sites at the surface of transition aluminas and are formed for dehydration at relatively high temperatures.

By the combined use of microgravimetry and of an early application of computer band resolution, also some quantitative aspects of the adsorption of py onto $\eta$-$Al_2O_3$ were considered by the same authors [68,72]. Some interesting points are:

(i) The maximum overall uptake of the strong base py is, with only minor differences between mildly and highly dehydrated specimens, of the order of ca. 3 py molecules per $nm^2$. After py

evacuation at 300 K, a condition often adopted by surface chemists, the overall uptake reduces to ca. 2 py molecules per $nm^2$ in the case of highly dehydrated alumina and to appreciably less than 2 in the case of mildly dehydrated aluminas. The maximum uptake figure is quite high if compared with the uptake of all other adspecies (except water) but the corresponding coverage does not go beyond a 0.2–0.3 fraction of a monolayer (i.e, approximately 1/3 of the average surface cation positions). This datum is not surprising: considering that most of the py adspecies form through a charge-release mechanism (lone-pair $\sigma$-donation to cus cations), relatively low coverages are expected, alumina being an insulating system and its capacity to lodge extra charge quite limited.

(ii) The maximum concentration of the weakest Lewis species $[py\text{-}L]_o$ is in the order of 1 py molecule per $nm^2$ (on highly dehydrated systems) and reduces to less than half that much by mere evacuation of adsorbed py at 300 K. These low figures imply that this adspecies is unfavored, in spite of the high number of $Al^{VI}_{cus}$ expected to be present on the basis of any dehydration model one wants to consider. It is unfavored as a consequence of its own weakness (i.e., the low uncoordination degree of a site $Al^{VI}_{cus}$) and as a consequence of the strong inductive effects deriving from the presence of other stronger Lewis coordinated adspecies.

(iii) The maximum concentration of the strongest $[py\text{-}L]_t$ Lewis adspecies is in the order of ca. 0.6 py molecules per $nm^2$, remains unchanged for py evacuation at up to ca. 500 K and reduces to ca. 0.4 for py evacuation at 573 K. On the basis of any 'ordered' dehydration model a much higher concentration of $Al^{IV}_{cus}$ sites should be expected at the surface of highly dehydrated aluminas (for instance, there should be ca. 1.75 $Al^{IV}_{cus}$ sites on the bare [111] crystal plane [35,68]) and a strong base like py should be capable of testing them all or nearly so. The adsorption of py so indicates, as does the adsorption of other weaker bases, that during dehydration at high temperatures reconstruction and ion shielding effects occur so that the concentration of highly uncoordinated sites is appreciably reduced [18,19]. The figure reported above for the $[py\text{-}L]_t$ adspecies also imply that the most reactive 'X-sites' [16], responsible for the $\alpha$-pyridone surface reaction, represent approximately 1/3 to 1/5 of the overall concentration of strong $Al^{IV}_{cus}$ sites revealed by py adsorption.

The scheme of interpretation of the complex $py/Al_2O_3$ system proposed by Morterra et al. [31,68] has seemed, since its proposal, quite realistic. This model is normally used as a reference by most authors that still deal in former years with the surface acidity of Al oxidic systems (mainly doped aluminas) as revealed by the adsorption of py.

Only Busca et al., in recent years, working with various non defective spinels as well as with the defective spinel $\delta$-$Al_2O_3$ [23], arrived to the conclusion that the Lewis coordinated py adspecies whose 8a ring mode is at 1610–1620 $cm^{-1}$ $(py\text{-}L]_{o,t}$) could have an alternative interpretation. Being this py adspecies virtually absent on non-defective spinels ($NiAl_2O_4$ and $CoAl_2O_4$), it may be attributed to a site involving an $Al^{IV}_{cus}$ ion, as suggested by Morterra et al. [68], but in a configuration that can be present only in the case of defective spinel structures. The site was identified by Busca with a structure of the type $[\square\text{–O–}Al^{IV}_{cus}]$, i.e., a cus $Al^{IV}$ ion carrying in its coordination sphere one of the cation vacancies imposed to the spinel structure by the $Al_2O_3$ stoichiometry: the cation vacancy would impose to the other oxide ions surrounding the $Al^{IV}$ ion a higher basicity, so that this Lewis acidic site is expected to withdraw charge from adsorbing bases less strongly than in the case of a regular $Al^{IV}_{cus}$ center.

### 5.2. *The adsorption of weak bases*

At ambient temperature, weak Lewis bases adsorb at the surface of oxides only onto the strongest Lewis acid sites, yielding low coverages and, in general, weak IR spectra.

If strong Lewis bases, like ammonia or py dealt with in the previous section, were able to differentiate all the families of acidic centers present at the surface of an oxidic system (see, for instance, the case of the three families of Lewis acid sites revealed by py on transition aluminas) there would be no need for studying the adsorption–desorption features of weak bases. But experience indicates that all the families of acidic sites, that are revealed by the use of strong bases, can be heterogeneous and can present, within each family, differences of acidity that the adsorption of strong bases is unable to show.

For this reason the adsorption of weak Lewis bases is, in principle, useful and is very frequently resorted to in addition to the adsorption of strong bases. The possible heterogeneity of the families of weak acid sites, that are unable to adsorb weak bases, is bound to remain unresolved, but the heterogeneity of the families of strong acid sites will be potentially resolved, if the weak bases adopted present a sufficient sensitivity to small differences of acidity.

In the case of Al oxides, the weak Lewis bases that have yielded a valuable contribution to the surface characterization of the various alumina systems are carbon monoxide and (linearly held) carbon dioxide. Some of the results obtained with these two weak bases will be reviewed separately.

*5.2.1. The adsorption of carbon monoxide*

At ambient temperature, CO does not adsorb at all on the Al oxidic systems in which Al ions present only the octahedral coordination (boehmite, corundum), whereas it adsorbs in small amounts on the Al oxidic systems in which also the tetrahedral coordination is allowed to Al ions. This confirms the importance of $Al^{IV}_{cus}$ centers for the development of strong acidity at the surface of Al oxides.

The ambient temperature adsorption of CO onto transition phase aluminas has been studied by several authors since the earliest days of IR spectroscopy applied to surface science (e.g., see [24,26,47,73,74]) and also in more recent years the interaction of CO with aluminas has been investigated both at ambient temperature and at low temperatures [18,19,36,75–77].

It is normally accepted by the researchers that, at ambient temperature, CO gives, on transition aluminas (as well as on most non-d metal oxides), a weak interaction of the acid–base type as a consequence of a polarization of the molecule and/or a small charge release from the $5\sigma$ lone pair orbital, mainly localized on the C atom. As the $5\sigma$ lone pair orbital has a partial antibonding character, CO adsorption brings about an increase of the $\nu_{CO}$ stretching frequency, whose extent measures the strength of the acid–base interaction.

Few exceptions have been reported to this behavior for the CO-transition aluminas system. For instance, Padley et al. [78] reported that on their $\gamma$-$Al_2O_3$ specimen, activated at relatively low temperatures, CO uptake at ambient temperature did not yield any coordinated CO adspecies, whereas surface carbonates were formed. The purity of that alumina was not reported; pure laboratory transition aluminas have then been checked again several times and no carbonates were ever observed by us to form, even in the presence of oxygen or air.

On the basis of the various works in the literature, in particular of the most recent contribution by Morterra et al. [19], the ambient temperature adsorption of CO on transition aluminas can be summarized to lead to the following:

(i) The activity of all transition phase aluminas towards CO begins only after activation at $T \geq 673$ K, i.e., after the elimination of over 60–70% of the surface hydrated layer (see Fig. 9) and the onset of the formation of defect sites in which multiple anion vacancies are present, according to all 'ordered' dehydration schemes [35]. CO does not probe, at ambient temperature, 'regular' $Al^{IV}_{cus}$ sites, but only particularly uncoordinated sites, possibly made up of clusters of $Al_{cus}$ ions, among which $Al^{IV}$ ions must be present.

(ii) On the low-temperature transition phase $\gamma$-$Al_2O_3$, three CO $\sigma$-coordinated adspecies are formed. Following the temperature of sample activation and the overall CO coverage, the $\nu_{CO}$ stretching frequency of the three adspecies is at 2195–2210 $cm^{-1}$ (species $(CO)_A$), 2215–2220 $cm^{-1}$ (species $(CO)_B$) and 2235–2240 $cm^{-1}$ (species $(CO)_C$). Fig. 12 shows the spectra and other spectral features of CO adsorbed at 300 K on a $\gamma$-$Al_2O_3$ specimen activated at 1023 K.

The two higher frequency CO adspecies ($(CO)_C$ and $(CO)_B$) have been assigned to two families of sites involving $Al^{IV}_{cus}$ ions located in crystallographically defective configurations and the lower frequency CO adspecies ($(CO)_A$) to sites involving particularly exposed $Al^{IV}_{cus}$ ions located in extended patches of regular low-index crystal planes.

The assignment was based on several arguments [19,77]. Two aspects of that assignment are worthwhile reporting here:

- The high frequency CO adspecies, especially the highest $\nu$ species $(CO)_C$, reach on dehydrated samples an intensity that is relatable to the intensity exhibited, in higher hydration stages, by the OH species absorbing at 3775 $cm^{-1}$. This correlation was already anticipated in Fig. 6 for a $\eta$-$Al_2O_3$ specimen. The OH band at 3775 $cm^{-1}$ was reported to be most likely ascribable to highly exposed $Al^{IV}$–OH groups located in crystallographically defective configurations. Also for the Lewis acid sites responsible for the $(CO)_C$ adspecies the most probable location is in crystallographically defective configurations.

- The adsorption of CO at ca. 77 K brings about, as expected, a fair increase of the overall CO uptake (Fig. 13 reports the CO adsorption at

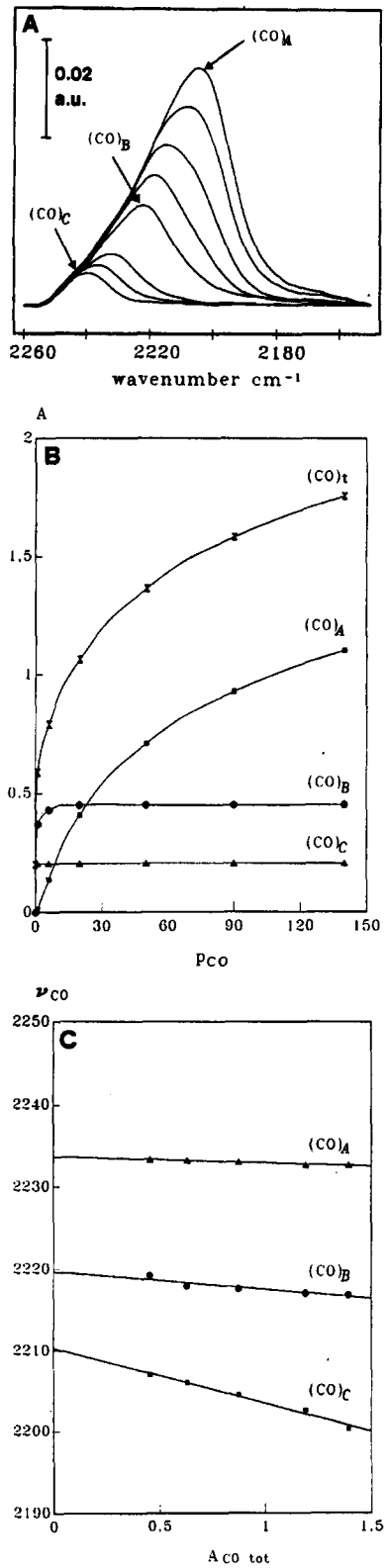


Fig. 12. Spectral features of CO adsorbed at 300 K on $\gamma$-$Al_2O_3$ activated at 1023 K. Section A: the absorbance spectra for CO uptake in the pressure range $1.4\times10^{2}-1.5\times10^{-2}$ Torr, section B: optical adsorption isotherms for the three resolved species $(CO)_A$, $(CO)_B$, and $(CO)_C$ and for the total $(CO)_t$ uptake, section C: depends of the individual CO frequencies on the overall CO coverage.

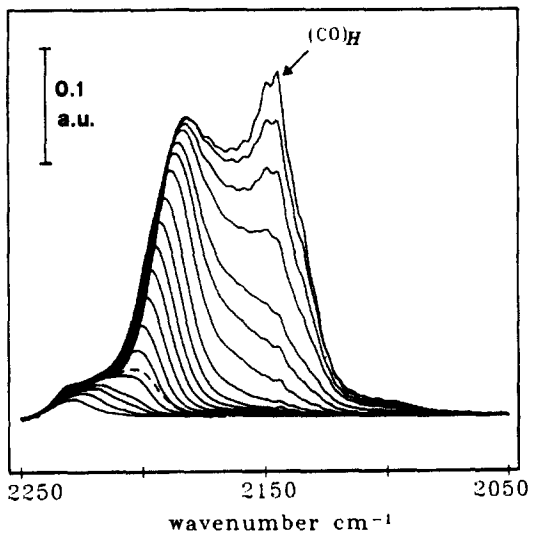


Fig. 13. The spectra of CO adsorbed at ca. 77 K onto $\gamma$-$Al_2O_3$ activated at 1023 K ($P_{CO}$ varies in the range $1\times10^{-3}$–$4\times10^{1}$ Torr).

ca. 77 K on the same sample of $\gamma$-$Al_2O_3$ described in Fig. 12).

The increased CO uptake is partly due to the appearance of a weak interaction of the H-bonding type with some residual OH groups ($(CO)_H$), but most of the increase is due to a ca. 20-fold growth of the $(CO)_A$ adspecies. The intensity of the other two more energetic species $(CO)_B$ and $(CO)_C$ remains virtually unchanged. This indicates that, at ambient temperature, the few strongest Lewis sites located in defective configurations are already saturated with CO (note in Fig. 12B the Langmuirian shape of the relevant adsorption isotherms), whereas only a small fraction of the abundant Lewis centers located on the regular crystal planes is saturated.

(Parenthetically, it is worthwhile mentioning here that the abundant adsorption of CO at ca. 77 K, especially the fraction due to the species $(CO)_A$, is responsible for the relaxation of surface $\nu_{Al-O}$ vibrations discussed in an earlier section and described in Fig. 2).

The other low-temperature transition phase alumina ($\eta$-$Al_2O_3$), that is normally regarded as more acidic than $\gamma$-$Al_2O_3$, exhibits stronger $(CO)_A$ and $(CO)_C$ bands [24], whereas the $(CO)_B$ species is hardly observable. The strongest $(CO)_C$ adspecies reaches, on $\eta$-$Al_2O_3$, $\nu_{CO}$ frequencies as high as ca. 2243 $cm^{-1}$, i.e., the highest $\nu_{CO}$ frequency observed on non-d metal oxides (see, for instance, Fig. 6B).

(iii) On high-temperature transition aluminas, mainly two $\sigma$-coordinated CO adspecies form. Fig. 14 shows the spectra and other spectral features of CO adsorbed at 300 K on a $\theta$-$Al_2O_3$ specimen activated at 1023 K.

Consistent with the increased crystalline order of the high-temperature spinel phases and with the larger average crystallite size [6,18,19], the strongest and most defective sites responsible for the strong species $(CO)_C$ have virtually disappeared, whereas the second family of defective sites responsible for the species $(CO)_B$ is still present. But the relative intensity of band $(CO)_B$ (strong Lewis sites in crystal defects) with respect to band $(CO)_A$ (strong Lewis sites on crystal planes) has reduced to ca. 1/3 of the relative intensity exhibited by $\gamma$-$Al_2O_3$ (compare the isotherms in Fig. 14B and 12B and the CO coverage figures reported below).

Also some quantitative aspects of CO uptake at ambient temperature onto transition aluminas have been considered [19,24,35,42]. The concentration of strong Lewis acid centers turned out to be, as expected, quite low and distributed as follows: (i) On $\gamma$-$Al_2O_3$ activated at 773 K, the overall CO uptake is of the order of ca. 0.1 mol/$nm^2$ (mainly ascribable to $(CO)_A$), whereas after activation at 1023 K the overall uptake becomes ca. 0.23 mol/$nm^2$. The distribution is: ca. 0.14 mol/$nm^2$ $(CO)_A$, ca. 0.06 mol/$nm^2$ $(CO)_B$ and ca. 0.03 mol/$nm^2$ $(CO)_C$. On $\eta$-$Al_2O_3$ activated at high temperature, the overall uptake is somewhat larger and in particular the strongest adspecies $(CO)_C$ reaches a concentration up to four times larger than on $\gamma$-$Al_2O_3$. (ii) On $\theta$-$Al_2O_3$ the overall uptake is larger than on $\gamma$-$Al_2O_3$ after activation at 773 K (ca. 0.14 mol. per $nm^2$), as a consequence of a faster dehydroxylation of high-temperature transition phases, whereas it is virtually coincident with that of $\gamma$-$Al_2O_3$ after activation at 1023 K (ca.

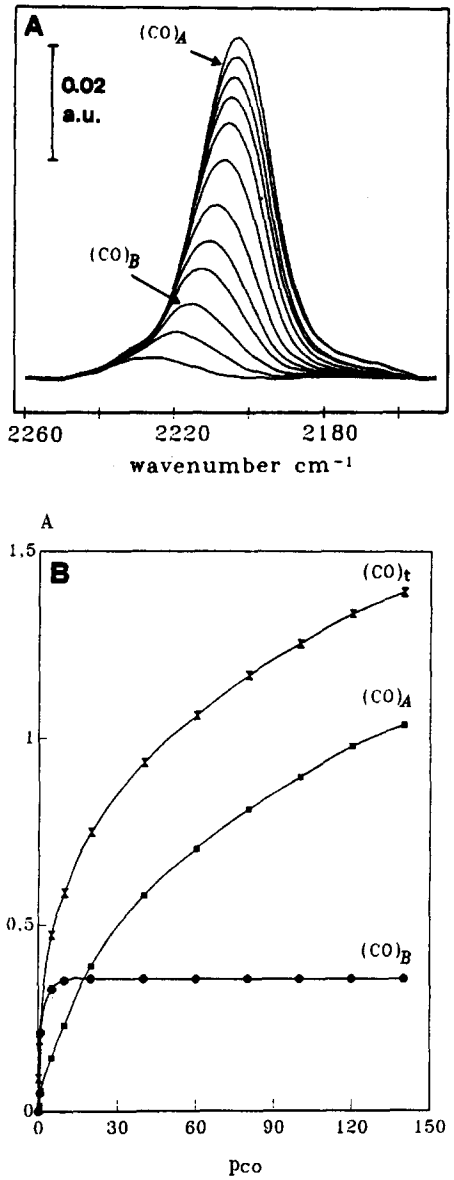


Fig. 14. Spectral features of CO adsorbed at 300 K on $\theta$-$Al_2O_3$ activated at 1023 K. Section A: the absorbance spectra for CO uptake in the pressure range $1.4\times10^{2}$–$1.5\times10^{-2}$ Torr, section B: optical adsorption isotherms for the two resolved species $(CO)_A$ and $(CO)_B$ and for the total $(CO)_t$ uptake.

0.22 mol. per $nm^2$). The latter figure is so distributed: ca. 0.17 mol/$nm^2$ for the 'regular' adspecies $(CO)_A$ and ca. 0.05 mol/$nm^2$ for the 'defective' adspecies $(CO)_B$ (and negligible amounts of species $(CO)_C$).

These quantitative figures, mainly derived from the combined use of gas-volumetric and IR spectroscopic measurements, are in fair agreement with other data of different origin: (i) the maximum concentration of Fink's 'X-sites' was estimated by Knözinger and Ratnasamy [35] to be in the order of ca. 0.1 sites per $nm^2$. This figure corresponds roughly to the concentration of the strongest Lewis sites located on crystal defects ($(CO)_B$ and $(CO)_C$); (ii) the maximum concentration of py strongly chemisorbed onto the $Al^{IV}_{cus}$ sites (8a py ring mode at ca. 1625 $cm^{-1}$) is 3–4 times larger than the maximum overall CO uptake obtainable at 300 K on the same material. And in fact, on both $\gamma$- and $\eta$-$Al_2O_3$ [72], it was found that py preadsorption inhibits completely the 300 K adsorption of all species of CO. Moreover, all of the py adspecies $[py\text{-}L]_o$ and $[py\text{-}L]_{o,t}$ must be thermally desorbed and more than half the amount of the strongest py adspecies $[py\text{-}L]_t$ must be thermally desorbed before any CO adsorption capacity can be gradually recovered.

In this respect, CO adsorption at ambient temperature has revealed to be quite successful in resolving the heterogeneity of the family of strongest Lewis acid sites, as revealed by py uptake: one family of strong Lewis acid sites (yielding $[py\text{-}L]_t$) is resolved, by CO uptake, in up to three sub-families characterized by different acidic strength.

### 5.2.2. *The adsorption of carbon dioxide*

It is well known that, on most metal oxides, $CO_2$ interacts at ambient temperature yielding, besides the so called carbonate-like species (dealt with in a previous section), also end-on $CO_2$ complexes [45,79]. This interaction occurs at surface uncoordinated cations (Lewis acid sites) by $\sigma$-charge release from one of the O lone pair orbitals, so that the molecule loses the center of symmetry, still preserving its linear shape ($D_{\infty h} \rightarrow C_{\infty v}$). Spectroscopically, the consequences of this interaction are the appearance of strong band(s) in the 2400–2300 $cm^{-1}$ range, due to the intense $\Sigma_u^+$ vibration ($\nu_3$) and of weak band(s) in the 1400–1370 $cm^{-1}$ range, due to the partial activation of two IR-forbidden

Fermi-resonant $\Sigma_g^+$ modes ($\nu_1$ and $2\nu_2$) [80]. The linear $CO_2$ adspecies are usually almost completely reversible at ambient temperature and were thus long considered as physisorbed species. Simple considerations on the $P_0$ value of $CO_2$ at ambient temperature and on the suppression of this adspecies upon preadsorption of strong Lewis bases ($H_2O$, py) clearly indicate that $CO_2$ molecules linearly held at the surface of oxides are indeed acid–base chemisorbed species.

In general terms, the end-on adsorption of $CO_2$ at ambient temperature is fairly similar to the $\sigma$-coordination of CO at the same temperature and should thus be expected to yield similar information. Actually, in the particular case of aluminas, end-on $CO_2$ uptake turns out to involve more families of surface cationic sites than CO and so yields complementary information.

Fig. 15 reports IR spectra of the adsorption of linear $CO_2$ on various Al oxidic systems.

The indications from the spectra of Fig. 15 can be summarized as follows: (i) The adsorption of linear $CO_2$ occurs in small amounts also at the surface of materials merely evacuated at ambient temperature. This indicates that, on aluminas, also the few cus cationic sites obtained by vacuum removal of coordinated undissociated water, one of the usual components of the surface hydrated layer, are Lewis acid sites sufficiently strong to polarize the $CO_2$ molecule. (ii) Linear $CO_2$ uptake on boehmite and corundum yields, after activation at any temperature compatible with the phase stability, a single band centered at 2340–2350 $cm^{-1}$ [14,49,79]. Considering that in these two systems Al ions possess only the octahedral coordination, the band is assigned to $Al^{VI}_{cus}$ sites. The presence of a sharp band at ca. 2345 $cm^{-1}$ also on transition aluminas activated at very low temperatures (see curve b in Fig. 15) indicates that, on spinel aluminas, $CO_2$ can adsorb also on the $Al^{VI}_{cus}$ sites, that cannot chemisorb CO. It is also deduced that, on transition phase aluminas, the earliest stages of dehydration (elimination of

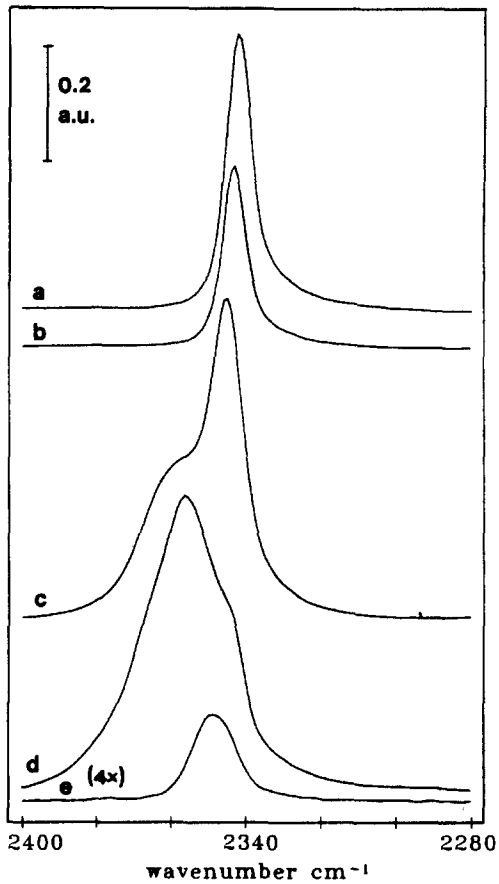


Fig. 15. Spectra of end-on surface complexes of $CO_2$ on various Al oxides ($P_{CO_2}$ = 12 Torr). (a) $\gamma$-AlOOH activated at 300 K, (b–c) $\gamma$-$Al_2O_3$ activated at 373 and 773 K, (d) $\theta$-$Al_2O_3$ activated at 1023 K, (e) $\alpha$-$Al_2O_3$ activated at 1023 K.

coordinated water and, possibly, of the first OH couples) involve prevalently surface $Al^{VI}$ ions. (iii) On transition aluminas activated at $T > 573$ K, two more bands of quite different intensity form at ca. 2370 $cm^{-1}$ (fairly strong, always observed) and ca. 2407 $cm^{-1}$ (very weak, sometimes not observed). These species present much higher resistance to evacuation [26,43,47]. These bands have been shown to involve $Al^{IV}_{cus}$ sites and precisely the highly defective sites responsible for the complex absorption of CO observable at ambient temperature. In fact, the competitive adsorption of an excess CO onto preadsorbed $CO_2$ was shown to desorb the stronger end-on $CO_2$ complexes and to convert them

reversibly into bridging carbonate structures [43].

Also on a quantitative ground, the correspondence between sites yielding strong end-on $CO_2$ complexes and CO $\sigma$-complexes is demonstrated by the observation that, on highly dehydrated transition aluminas, up to ca. 0.5 mol $CO_2/nm^2$ are adsorbed reversibly at 300–373 K (i.e., are $CO_2$ adspecies other than carbonate-like structures, that require higher temperatures for desorption).

*5.2.3. The adsorption of hydrogen*

A particularly interesting chapter of aluminas surface acid behavior, or better surface acid–base behavior, is represented by the chemisorptive interaction with hydrogen.

It has been known since a long time that transition aluminas can catalyze the o-p-$H_2$ conversion and the $H_2$–$D_2$ equilibration at low temperatures, if the oxides have been activated at $T > 873$ K [50]. It is also known that in no activation conditions can $\alpha$-$Al_2O_3$ catalyze any of the mentioned reactions.

These observations indicate, on the basis of the discussion carried out in the previous sections, that the mentioned reactions should involve few active sites of highly defective nature, involving (at least one) $Al^{IV}_{cus}$ site. The exceptional nature (i.e., the highly defective nature) of the sites active in $H_2$ conversion and equilibration reactions was postulated also by the authors quoted above [50] who examined the phenomenon from a catalytic and kinetic point of view.

The adsorption of $H_2$ on activated transition aluminas has been studied in quantitative terms by Amenomiya several years ago [81] and some aspects of the $H_2$/alumina interaction are still being examined in these years [42]. It is normally observed that the total number of sites active for $H_2$ chemisorption does not exceed the figure of ca. 0.2 centers/$nm^2$. This is a number closely comparable with that of Fink's 'X-sites' and with the figure corresponding to the Lewis acid sites active towards CO at 300 K as well as to the strongest fraction of sites active towards py.

Amounts and types of adsorbed $H_2$ strictly depend on contact temperature. The most important types of adsorbed $H_2$ observed by Amenomiya [81] were: (i) an associated form, adsorbed and desorbed at 77 K, termed H(P) and ascribed by Amenomiya to a physical adsorption; (ii) a species, termed H(I), formed dissociatively at 198 K and desorbed fast at the same temperature. This species was thought not to involve 'X-sites' and was considered to involve ca. 0.1 sites per $nm^2$; (iii) another species, adsorbed dissociatively and very slowly at ambient temperature (298–373 K), was termed H(III) and was supposed to involve approximately 0.2 sites/$nm^2$; (iv) a last species, termed H(V) and involving the same amount of surface sites, formed only at $T > 573$ K, when all other $H_2$ adspecies are either left in negligibly small amounts or have already desorbed.

For many years all forms of adsorbed $H_2$ could not be observed spectroscopically, although at least some of them should lead to the appearance in the IR spectrum of Al–H and new O–H stretching bands. In 1978 Knözinger and Ratnasamy in their review [35] still reported the lack of any spectral evidence for adsorbed $H_2$, claiming that 'no really adequate experiments seemed to have been performed'.

Successively, only Kazansky and co-workers [82,83], using an accurate in situ diffuse reflectance technique, succeeded in observing in the IR spectrum of $\eta$-$Al_2O_3$ (and other oxidic materials, including zeolites) several forms of adsorbed $H_2$.

Kazansky's observations relative to the $H_2/\eta$-$Al_2O_3$ system can be summarized as follows:

(i) Fig. 16A reports the spectrum of molecular (undissociated) $H_2$, adsorbed at 77 K on $\eta$-$Al_2O_3$ activated at 973 K.

There are three bands, centered at 3975, 4020 and 4105 $cm^{-1}$. The latter band, exhibiting the slightest downwards shift with respect to the (IR inactive) $\nu_{H-H}$ vibration of molecular hydrogen

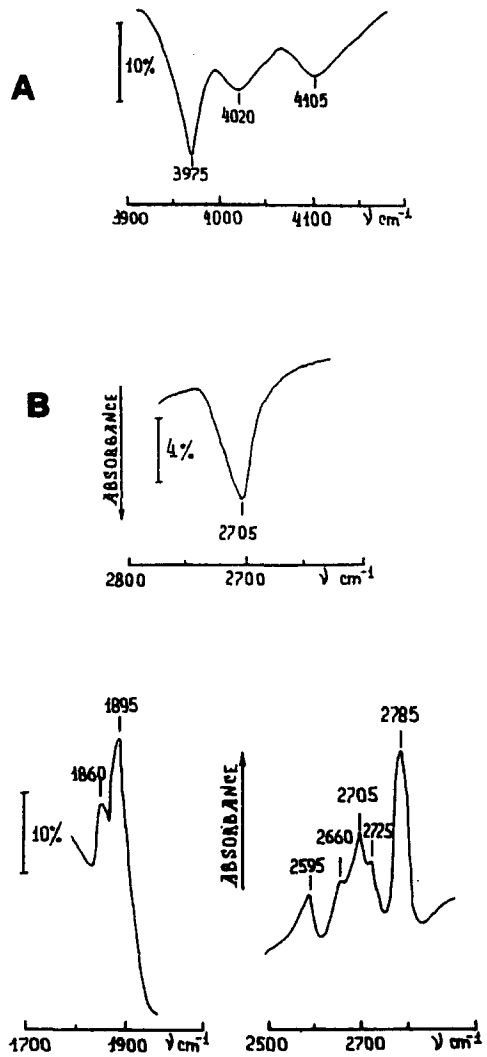


Fig. 16. Spectral features of $H_2$ ($D_2$) adsorbed, at various temperatures, onto activated $\eta$-$Al_2O_3$. Section A: $H_2$ adsorbed at 77K, section B: $D_2$ adsorption at 180 K, section C: $H_2$ adsorption (left-hand segment) and $D_2$ adsorption (right-hand segment) at 300 K. (From Ref. [82,83].

(4160 $cm^{-1}$ [84]), was ascribed to $H_2$ molecules weakly interacting with surface OH groups, as demonstrated by the decreasing intensity of the band with increasing activation temperature.

The bands at lower frequency, which appear only after alumina pretreatment at $T > 770$ K, were ascribed by Kazansky to $H_2$ molecules held by aprotic sites, formed in the course of the high temperature dehydroxylation. In particular, the strongest $H_2$ adspecies absorbing at 3975 $cm^{-1}$ was found to correspond in concentration to the 'X-sites' and to be completely inhibited by the room temperature preadsorption of CO, namely by the fraction yielding the strongest CO adspecies absorbing at ca. 2245 $cm^{-1}$ [24].

The spectra of Kazansky conclusively demonstrate that, at 77 K, molecular $H_2$ exists at the surface of transition aluminas in three specifically adsorbed forms and not as a physisorbed (aspecific) phase, as postulated by Amenomiya [81].

(ii) Using $D_2$ uptake, Amenomiya's species H(I) (D(I)) was observed to form dissociatively at 180–240 K and to lead to the appearance of an OD vibration at 2705 $cm^{-1}$, as shown in Fig. 16B. The relevant sites were confirmed to be very few and to be different from the so-called 'X-sites', as no inhibition was produced on H(I) adsorption by the preadsorption of CO at ambient temperature. The new-formed OD species absorbing at 2705 $cm^{-1}$ was found to undergo very fast exchange with $H_2$ and $CH_4$ [83].

(iii) The slow chemisorbed form termed by Amenomiya H(III) was observed by Kazansky to occur at $T > 240$ K and to yield several bands in the $\nu_{Al-H}$ stretching region and, using $D_2$, in the $\nu_{O-D}$ stretching region. This is shown in Fig. 16C. The occurrence of the species H(III) on the usual family of very strong Lewis acid sites termed 'X-sites' (and, obviously, on nearby cus oxide ions) is demonstrated by the fact that, when the room temperature chemisorption of $H_2$ ($D_2$) is completed, no CO chemisorption in the strongest form (i.e., the $(CO)_C$ band centered at ca. 2245 $cm^{-1}$) occurs anymore.

(iv) The formation of Amenomiya's species H(V) could be observed by Kazansky only in a more indirect way. In fact, at temperatures as high as 500 K, the dissociative chemisorption of $H_2$ ($D_2$) did not produce Al–H or O–D stretching bands different from those typical of the species H(III), but was accompanied by the formation of some far more stable aluminum hydride species, still absorbing at the same frequencies of species H(III) and shown in Fig.

16C. It was so deduced that the high temperature $H_2$ adsorption, that is still a dissociative one, is accompanied by some surface mobility processes, leading to a rearrangement of the surface complexes and resulting in their higher stability.

After the experiments by Kazansky were published, no other authors reported observing IR spectral evidence for $H_2$ chemisorption on transition aluminas. This is most likely due to the high sensitivity guaranteed, in some spectral regions and with some highly scattering powdery materials, by the diffuse reflectance technique. As for the low temperature molecular form of chemisorbed $H_2$, other authors (including the ones writing this review) tried with no success to reproduce Kazansky's data using other types of low-temperature IR cells (e.g., see Ref. [18]). Their failure is most likely due to the sample temperature, definitely higher than 77 K, usually reached in the transmission low-temperature cells, as opposed to the actual 77 K temperature obtainable in Kazansky's set-up, in which the sample is completely immersed in liquid nitrogen.

## 6. Conclusive remarks

Aim of this review was not the description of the enormous amount of IR spectroscopic work that has been devoted, in the years, to the adsorption onto catalytic aluminas of various probe molecules and/or various reagents of possible catalytic reactions. Systematic information of this kind was reported, up to some ten years ago, in previous reviews (that have been frequently referred to in this work) and the completion of that type of information is nowadays easily accessible through the use of on-line international data bases.

Our purpose was rather that of describing the state of our present knowledge on some of the most important surface features of catalytic aluminas, as obtained by the use of IR spectroscopy. Doing so, we tried to pay some attention also to the historical evolution of this knowledge through some thirty years of research. We also tried to involve, in the description, the minimum number of selected adsorbed species, as the comprehension of the surface behavior of the alumina systems was our ultimate goal and was believed to be more important than the detailed description of how it was obtained.

The overall picture that comes out of this work is, in general terms, quite complete and consistent. Nonetheless, there are still some residual controversial aspects (e.g., consider the ultimate assignment of (some) surface OH species) and some surface chemical aspects of catalytic aluminas are still not thoroughly understood. Among the latter, the most important one is certainly connected with the actual atomic-scale nature of the catalytic sites: we know the order of magnitude of their (maximum) amount, we know the conditions in which they form, we know that they must involve $Al^{IV}$ centers and are most likely localized in crystallographically defective configurations, but we do not know exactly which surface atoms and how many surface atoms are involved in each active site.

In spite of the remaining uncertainties, it is our opinion that a guide line can be derived from the various chapters of this review to choose, for a catalysis work with aluminas, the best alumina phase and the best physical and/or chemical preliminary treatment of the catalytic alumina. In particular, we think that the overall picture here obtained for the surface properties of transition aluminas may be of some help for the understanding of the surface behavior of those Al oxidic systems that are still being systematically investigated in these years, i.e., the catalytic aluminas surface modified with cationic and/or with anionic dopants.

## References

[1] R. Marshall, S.S. Mitra, P.J. Gielisse, J.N. Plendl and L.C. Mansur, J. Chem. Phys., 43 (1965) 2893.

[2] B.C. Lippens and J.J. Steggerda, in B.G. Linsen (Editor), Physical and Chemical Aspects of Adsorbents and Catalysts, Academic Press, New York, 1970, p. 171.
[3] B.C. Lippens, Thesis, Delft, 1961.
[4] S. Soled, J. Catal., 81 (1983) 252.
[5] F. Abbatista, S. Del Mastro, G. Gozzelino, D. Mazza, M. Vallino, G. Busca, V. Lorenzelli and G. Ramis, J. Catal., 117 (1989) 42.
[6] P. Nortier, P. Fourre, A.B. Mohammed Saad, O. Saur and J.C. Lavalley, Appl. Catal., 61 (1990) 141.
[7] M.C. Stegmann, D. Vivien and C. Manziéres, J. Chim. Phys., 71 (1974) 761.
[8] S.J. Wilson and J.D.C. McConnell, J. Solid State Chem., 34 (1980) 315.
[9] S.J. Wilson, Proc. Brit. Ceram. Soc., 28 (1979) 281.
[10] M.I. Baraton and P. Quintard, J. Mol. Struct., 79 (1982) 337.
[11] G. Busca, V. Lorenzelli, G. Ramis and R.J. Willey, Langmuir, 9 (1993) 1492.
[12] P. Tarte, Spectrochim. Acta, 23A (1967) 2127.
[13] A.B. Kiss, G. Keresztury and L. Farkas, Spectrochim. Acta, 36A (1980) 653.
[14] C. Morterra, C. Emanuel, G. Cerrato and G. Magnacca, J. Chem. Soc., Faraday Trans., 88 (1992) 339.
[15] C. Morterra, in Proc. 6th Int. Congr. Catal. (London 1976), 1976, p. 194.
[16] H. Knözinger, H. Krietenbrink, H.D. Muller and W. Schultz, in G.C. Band, P.B. Wells and F.C. Tompkins (Editors), Proc. 6th Int. Congr. Catal. (London 1976), 1976, p. 183.
[17] J.C. Lavalley and M. Benaissa, J. Chem. Soc., Chem. Comm., (1984) 908.
[18] L. Marchese, S. Bordiga, S. Coluccia, G. Martra and A. Zecchina, J. Chem. Soc., Faraday Trans., 89 (1993) 3483.
[19] C. Morterra, V. Bolis and G. Magnacca, Langmuir, 10 (1994) 1812.
[20] L.H. Little, in Infrared Spectra of Adsorbed Species, Academic Press, London, 1966, p. 228.
[21] (a) A.A. Tsyganenko and V.N. Filimonov, Spectrosc. Lett., 5 (1972) 477; (b) A.A. Tsyganenko and V.N. Filimonov, J. Mol. Struct., 19 (1973) 579.
[22] J.B. Peri, J. Phys. Chem., 69 (1965) 220.
[23] G. Busca, V. Lorenzelli, V. Sanchez Escribano and R. Guidetti, J. Catal., 131 (1991) 167.
[24] G. Della Gatta, B. Fubini, G. Ghiotti and C. Morterra, J. Catal., 43 (1976) 90.
[25] C. Morterra, A. Chiorino, G. Ghiotti and E. Garrone, J. Chem. Soc., Faraday Trans. 1, 75 (1979) 271.
[26] (a) N.D. Parkyns, J. Chem. Soc. A, (1969) 410; (b) N.D. Parkyns, J. Phys. Chem., 75 (1971) 526.
[27] E. Baumgarten and A. Zachos, Spectrochim. Acta, 37A (1981) 757.
[28] J.C. Lavalley, M. Benaissa, G. Busca and V. Lorenzelli, Appl. Catal., 24 (1986) 249.
[29] C. Morterra, G. Ghiotti, E. Garrone and F. Boccuzzi, J. Chem. Soc., Faraday Trans. 1, 72 (1976) 2722.
[30] C. Morterra, G. Ghiotti, F. Boccuzzi and S. Coluccia, J. Catal., 51 (1978) 299.
[31] A. Zecchina, S. Coluccia and C. Morterra, Appl. Spectrosc. Rev., 21 (1985) 259.
[32] J.B. Peri, Disc. Faraday Soc., 52 (1971) 55.
[33] C. Morterra, G. Magnacca and N. Del Favero, Langmuir, 9 (1993) 642.
[34] G. Busca, V. Lorenzelli and V. Sanchez Escribano, Chem. Mater., 4 (1992) 595.
[35] H. Knözinger and P. Ratnasamy, Catal. Rev., Sci. Eng., 17 (1978) 31.
[36] T.H. Ballinger and J.T.Y. Yates Jr., Langmuir, 7 (1991) 3041.
[37] A. Iordan, M.I. Zaki and C. Kappenstein, J. Chem. Soc., Faraday Trans., 89 (1993) 2527.
[38] (a) J.M. Brown, J. Chem. Soc., Dalton Trans., (1972) 338; (b) P.A. Bulliner and T.G. Spiro, Inorg. Chem., 8 (1969) 1023.
[39] P. Berteau, M.A. Kellens and B. Delmon, J. Chem. Soc., Faraday Trans., 87 (1991) 1425.
[40] J. Shen, R.D. Cortright, Y. Chen and J.A. Dumesic, J. Phys. Chem., 98 (1994) 8067.
[41] C. Morterra, G. Magnacca, G. Cerrato, N. Del Favero, F. Filippi and C.V. Folonari, J. Chem. Soc., Faraday Trans., 89 (1993) 135.
[42] M. Cabrejas Manchado, J.M. Guil, A. Pérez Masia, A. Ruiz Paniego and J.M. Trejo Menayo, Langmuir, 10 (1994) 685.
[43] C. Morterra, A. Zecchina, S. Coluccia and A. Chiorino, J. Chem. Soc., Faraday Trans. 1, 73 (1977) 1544.
[44] K. Nakamoto, Infrared Spectra of Inorganic and Coordination Compounds, 2nd edition, Wiley, New York, 1970, p. 169.
[45] G. Busca and V. Lorenzelli, Mater. Chem., 7 (1982) 89.
[46] C. Morterra and L. Orio, Mater. Chem. Phys., 24 (1990) 247.
[47] (a) J.B. Peri, J. Phys. Chem., 70 (1966) 3168; (b) J.B. Peri, J. Phys. Chem., 72 (1968) 2917.
[48] S.J. Gregg and J.D.F. Ramsay, J. Phys. Chem., 73 (1969) 1243.
[49] C. Morterra, S. Coluccia, G. Ghiotti and A. Zecchina, Z. Phys. Chem. N.F., 104 (1977) 275.
[50] (a) P.C. Saunders and J.W. Hightower, J. Phys. Chem., 74 (1970) 4323; (b) F.H. Van Cauwelaert and W.K. Hall, Trans. Faraday Soc., 66 (1970) 454; (c) J.W. Hightower and W.K. Hall, Trans. Faraday Soc., 66 (1970) 477.
[51] J. Kijenski and A. Baiker, Catal. Today, 5 (1989) 1.
[52] A. Auroux and A. Gervasini, J. Phys. Chem., 94 (1990) 6371.
[53] H. Knözinger, Adv. Catal., 25 (1976) 184.
[54] J. Medema, J.G.M. Van Bokhoven and A.E.T. Kuiper, J. Catal., 25 (1972) 238.
[55] W.A. Pliskin and R.P. Eischens, J. Phys. Chem., 59 (1955) 1156.
[56] (a) J.B. Peri and R.B. Hannan, J. Phys. Chem., 64 (1960) 1526; (b) J.B. Peri, J. Phys. Chem., 69 (1965) 231.
[57] H. Dunken, P. Fink and E. Pilz, Chem. Tech. (Leipzig), 18 (1966) 490.
[58] A.A. Tsyganenko, D.V. Pozdhyakov and V.N. Filimonov, J. Mol. Struct., 29 (1975) 299.
[59] C.H. Kline and J. Turkevich, J. Chem. Phys., 12 (1944) 300.
[60] C. Morterra, A. Chiorino, G. Ghiotti and E. Fisicaro, J. Chem. Soc., Faraday Trans. 1, 78 (1982) 2649.
[61] E.P. Parry, J. Catal., 2 (1963) 371.

[62] A.V. Kiselev and A.V. Uvarov, Surface Sci., 6 (1967) 399.
[63] P. Pichat, M.V. Mathieu and B. Imelik, Bull. Soc. Chim. Fr., (1969) 2611.
[64] F.E. Kiviat and L. Petrakis, J. Phys. Chem., 77 (1973) 1232.
[65] O.F. Kirina, T.V. Antipina and G.D. Chukin, Russ. J. Phys. Chem., 47 (1973) 248.
[66] (a) H. Knözinger and H. Stolz, Fortschrittsber. Kolloide Polym., 55 (1971) 16; (b) H. Stolz and H. Knözinger, Kolloid Z. Z. Polym., 243 (1971) 71.
[67] P. Fink, Rev. Roum. Chim., 14 (1969) 811.
[68] C. Morterra, A. Chiorino, G. Ghiotti and E. Garrone, J. Chem. Soc., Faraday Trans. 1, 75 (1979) 271.
[69] C. Morterra, S. Coluccia, A. Chiorino and F. Boccuzzi, J. Catal., 54 (1978) 348.
[70] B.A. Morrow and I.A. Cody, J. Phys. Chem., 80 (1976) 1995.
[71] M. Kermarec, M. Briend-Faure and D. Delafosse, J. Chem. Soc., Faraday Trans 1, 70 (1974) 2180.
[72] C. Morterra, S. Coluccia, E. Garrone and G. Ghiotti, J. Chem. Soc., Faraday Trans. 1, 75 (1979) 289.
[73] L.H. Little and C.H. Amberg, Can. J. Chem., 40 (1962) 1997.
[74] C.E. O'Neil and D.J.C. Yates, J. Phys. Chem., 65 (1961) 901.
[75] (a) E.A. Paukshtis, R.I. Soltanov and E.N. Yurchenko, React. Kinet. Catal. Lett., 16 (1981) 93; (b) R.I. Soltanov, E.A. Paukshtis and E.N. Yurchenko, Kinet. Katal., 23 (1982) 164; (c) E.A. Paukshtis and E.N. Yurchenko, Russ. Chem. Rev., 52 (1983) 242.
[76] (a) M.I. Zaki and H. Knözinger, Mater. Chem. Phys., 17 (1987) 201; (b) M.I. Zaki and H. Knözinger, Spectrochim. Acta, 43A (1987) 1455.
[77] A. Zecchina, E. Escalona Platero and C. Otero Areán, J. Catal., 107 (1987) 244.
[78] M.B. Padley, C.H. Rochester, G.J. Hutchings and F. King, J. Catal., 148 (1994) 438.
[79] C. Morterra, G. Cerrato and C. Emanuel, Mater. Chem. Phys., 29 (1991) 447.
[80] G. Ramis, G. Busca and V. Lorenzelli, Mater. Chem. Phys., 29 (1991) 425.
[81] Y. Amenomiya, J. Catal., 22 (1971) 109.
[82] V.B. Kazansky, V. Yu. Borovkov and L.M. Kustov, Proc. of the 8th Int. Congr. on Catalysis (Berlin, West Germany, 1984), Vol. III, Verlag Chemie, Weinheim, p. 3.
[83] V.B. Kazansky, V. Yu. Borovkov and A.V. Zaitsev, in M.J. Phillips and M. Ternan (Editors), Proc. of the 9th Int. Congr. on Catalysis (Calgary, Canada, 1988), p. 1426.
[84] G. Herzberg, Molecular Spectra and Molecular Structure I. Spectra of Diatomic Molecules, Van Nostrand, Princeton, 1950, p. 62.